

# **Textile Electrodes In Electromyography Measurements For Hand Gesture Recognition**

**Arla Elina Aurora von Konow**

**School of Electrical Engineering**

Thesis submitted for examination for the degree of Master of  
Science in Technology.

Espoo 18.5.2020

**Thesis supervisor:**

Prof. Kari Halonen

**Thesis advisors:**

Post Doc. Elina Ilén

Asst. Prof. Ivan Vujaklija

Author: Arla Elina Aurora von Konow		
Title: Textile Electrodes In Electromyography Measurements For Hand Gesture Recognition		
Date: 18.5.2020	Language: English	Number of pages: 6+39
Degree Programme: Nano and Radio Sciences		
Major: Micro- and Nanoelectronic Circuit Design		Code: ELEC3036
Supervisor: Prof. Kari Halonen		
Advisors: Post Doc. Elina Ilén, Asst. Prof. Ivan Vujaklija		
<p>This thesis investigates the use of conductive textiles as the material of surface electromyography electrodes especially in the case of hand gesture recognition. Several conductive textile materials are used to design electrode setups integrated in sleeve to measure an 8-channel EMG signal around forearm. The electric properties of the electrodes are investigated and the EMG signal is used in a data classification experiment to assess the performance of the textile electrodes in gesture recognition compared to conventional medical grade electrodes. The design and manufacturing process is also described in order to underline all benefits and challenges associated with the materials and methods. This thesis shows that textile electrodes are a viable option for conventional wet gel electrodes in gesture recognition applications.</p>		
Keywords: Electronic textiles, e-textiles, smart textiles, intelligent clothing, electromyography, machine learning, motion recognition, human-machine interfacing		

Tekijä: Arla Elina Aurora von Konow

Työn nimi: Tekstiilelektrodit electromyografiamittauksissa

Päivämäärä: 18.5.2020

Kieli: Englanti

Sivumäärä: 6+39

Koulutusohjelma: Nano and Radio Sciences

Pääaine: Micro- and Nanoelectronic Circuit Design

Koodi: ELEC3036

Työn valvoja: Prof. Kari Halonen

Työn ohjaajat: Post Doc. Elina Ilén, Asst. Prof. Ivan Vujaklija

Tämä diplomityö tutkii johtavien tekstiilien soveltuvuutta pintaelektrodien materiaaliksi erityisesti mitattaessa lihasaktiivisuussignaalia (EMG) kyynärvarren lihaksista käden eleiden tunnistamista varten. Työssä mitataan elektrodien sähköisiä ominaisuuksia ja verrataan niitä perinteisiin klinisiin pintaelektrodeihin. Diplomityö esittää myös tekstiilien ja työtapojen vahvuuksia ja heikkouksia, jotka ilmenivät prototyyppien suunnittelu- ja valmistusprosessin aikana. Tulokset osoittavat, että tekstiilelektrodit soveltuvat erittäin hyvin käden eleiden tunnistamiseen pyrkiviin mittauksiin.

Avainsanat: puettava elektroniikka, e-tekstiilit, electromyografia, koneoppiminen, eleentunnistus

## Preface

I want to thank Professor Kari Halonen for the opportunity to work with interesting topics in his research group and providing me with an intriguing topic for my master's thesis. I also want to thank my two advisors, post doctoral researcher Elina Ilén for her insight in textiles and assistant professor Ivan Vujaklija for his expertise in electromyography and data classification. A big thank you to my colleague Samu Järvinen as well for collaborating with me in this project. I also had a great deal of help and support from my spouse Lauri who has an abundance of medical literature and knowledge and my sister Elsa who lent me a hand when mine was not working.

Otaniemi, 18.5.2020

Arla von Konow



# Contents

<b>Abstract</b>	<b>ii</b>
<b>Abstract (in Finnish)</b>	<b>iii</b>
<b>Preface</b>	<b>iv</b>
<b>Contents</b>	<b>v</b>
<b>Symbols and abbreviations</b>	<b>vi</b>
<b>1 Introduction</b>	<b>1</b>
<b>2 Background</b>	<b>2</b>
2.1 Basics of Electromyography . . . . .	2
2.2 Electrodes as Transducers . . . . .	4
2.3 Conductive Textiles In Biosensing . . . . .	5
2.4 Gesture Recognition . . . . .	5
<b>3 Design Process</b>	<b>7</b>
3.1 Materials and Manufacturing Methods . . . . .	7
3.1.1 Base Garment . . . . .	7
3.1.2 Conductive Fabrics . . . . .	7
3.1.3 Conductive Threads . . . . .	8
3.1.4 Stitching and Embroidering . . . . .	8
3.1.5 Electrode Dimensions . . . . .	12
3.2 Single electrode pairs . . . . .	12
3.3 Electrode Array Sleeves . . . . .	13
<b>4 Validation</b>	<b>16</b>
4.1 Impedance Spectroscopy . . . . .	16
4.1.1 Methods . . . . .	16
4.1.2 Results And Discussion . . . . .	17
4.2 Frequency Response . . . . .	19
4.2.1 Methods . . . . .	19
4.2.2 Results And Discussion . . . . .	20
4.3 EMG Acquisition Performance and Gesture Recognition . . . . .	24
4.3.1 Signal baseline and resistance to interference . . . . .	26
4.3.2 Maximum Voluntary Contraction . . . . .	26
4.3.3 Functional Gesture Recognition Test . . . . .	28
<b>5 Conclusion</b>	<b>34</b>

## Symbols and abbreviations

### Symbols

$Ag(s)$	silver (solid)
$Ag^+(aq)$	silver ion (dissolved in water)
$C_d$	electrode capacitance
$e^-$	electron
$E_{hc}$	electrode metal half-cell potential
$R_d$	electrode resistance
$R_s$	electrolyte resistance
V	volt
$\Omega$	ohm

### Abbreviations

AR	augmented reality
DC	direct current
EMG	electromyography
EMI	electromagnetic interference
FFT	fast fourier transform
HCI	human–computer interaction
IAP	intracellular action potential
MVC	maximum voluntary contraction
RMS	root-mean-square
TNR	true negative rate
TPR	true positive rate
VR	virtual reality

# 1 Introduction

Intelligent and smart clothing are phenomena that are gaining ground in sports, healthcare and every day life. They are clothing embedded with electronics that for example measure bio signals from the wearer's body or add functionality[1][2]. Finland has a number of competitive companies on the market, such as Reima ([www.reima.com](http://www.reima.com)), VTT ([www.vtt.fi](http://www.vtt.fi)) and Myontec ([www.myontec.com](http://www.myontec.com)). Reima has been investigating integration of electronics in clothing already in 1998 with their Cyberia project [3] and now they are monitoring the activity of children with the ReimaGO sensor [4]. Myontec develops smart clothing to improve occupational health and ergonomics and to analyze sports performance [5]. VTT has recently conducted a project called Smart Clothing 2.0 that was about creating business opportunities to Finnish smart clothing products [6].

Electromyography (EMG) studies the electrical activity of skeletal muscles [7]. The main biomechanical parameters that have been recorded using EMG include muscle activation timing, force and fatigue [8]. The data was utilized for example in ergonomic analysis when evaluating the working conditions in industry [9]. More recent applications include diagnostic and therapeutic purposes in dentistry [7]. The potential of EMG signal classification has also been researched in the field of Human Computer Interaction HCI. That is, interpreting the EMG signal to control a computer or a robotic limb. In addition to quality of life improving applications, this technology could also be used in interactive computer gaming. [10] Gaming and healthcare applications can also be combined, as demonstrated by a study that proposed using EMG as a control device for a video game to motivate rehabilitation patients [11]. Intelligent clothing featuring EMG measurement could provide comfortable, convenient and reusable solutions for these applications.

This thesis is a part of a larger biosensing platform development project in our research group. The main purpose of the thesis is to contribute to that project, but in a wider scope the aim of this thesis is to give a recommendation about the materials when constructing textile electrodes by providing information about the electrical properties of the currently available conductive textiles and their performance in measuring the surface EMG as electrodes integrated in clothing, specifically in gesture recognition experiments. This is accomplished by designing and manufacturing several prototypes, performing a variety of measurements and experiments on them and comparing the results with those of conventional wet gel electrodes.

In addition to studying the properties of the materials, this thesis describes the design process and the challenges faced during it. This contributes to the knowledge of what things have to be taken into consideration when manufacturing textile electrodes and what is the optimal work flow working with these materials.

There are five chapters in this thesis. Chapter 2 discusses the background of this thesis including the EMG signal generation, the concept of electrodes, overview of conductive textiles in biosensing and an introduction to gesture recognition. Chapter 3 presents the materials and methods used in the prototypes and the design process. Chapter 4 describes the measurement setups and presents and discusses the results. Chapter 5 summarizes the findings and makes propositions for future research.

## 2 Background

The first chapter introduced the concept of intelligent clothing, gave motivation for using EMG signal for gesture recognition and presented the goals of this thesis. This chapter delves into the background of EMG signal, electrodes, gesture recognition and conductive textiles. Before going to the step by step description of the generation of the EMG signal in human body, Section 2.1 explains the concept of an action potential, its propagation principles and the physiology and working principle of motor neurons. Section 2.2 is dedicated to electrodes that are the interface between the human body and the measurement device and Section 2.3 gives a general view conductive textiles, the material of which the electrodes under study of this thesis are made of.

### 2.1 Basics of Electromyography

Action potential is a short and fast change in the muscle cell membrane potential with a magnitude of approximately 100 mV depicted by Figure 1. The resting potential of a muscle cell membrane is approximately -70 mV. This means that the inside of a cell has a negative charge compared to the outside of the cell. After a triggering event (electrical, chemical or mechanical stimulus), the membrane potential starts to rise slowly until it reaches the threshold voltage at about -50 mV. Then the potential rapidly increases to 30 mV. Immediately after this period called depolarization, the membrane repolarizes. That is, the potential rapidly decreases causing a brief moment of hyperpolarization at -90 mV before returning to the resting potential of -70 mV. [12][13]

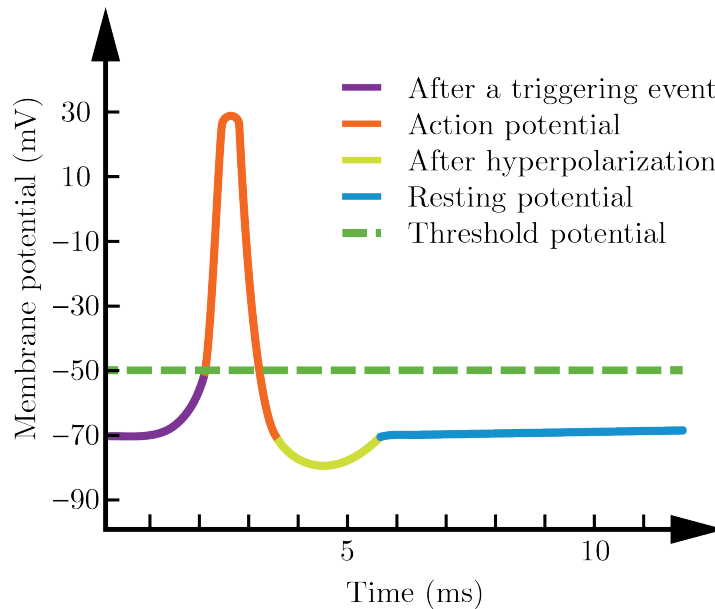


Figure 1: Cell membrane potential during action potential. Adapted from [12]

The action potential has a couple of interesting electrical properties: the lack of

attenuation or distortion in the signal and the nature of operating according to the so called all-or-none law. The action potential is actually identical at the starting point in the brain and in the nerve-muscle synapsis. This is possible, because unlike an electric signal traveling through a lossy wire, an action potential regenerates itself continuously by triggering a new, local and similarly shaped action potential in the neighboring section. In fact, once an action potential is initiated, it will always reach the same maximum value. This principle of function is called the all-or-none law. For this reason, the magnitude of the muscle stimulus cannot be determined by the magnitude of the incoming action potentials, but rather their frequency. [12] That property is called rate coding. In addition to that, the magnitude and direction of the force generated by a muscle also depends on the number of activated neurons, that is the recruitment. [14]

Motor neurons (Figure 2) are neurons that are used for controlling the skeletal muscles. One motor nerve consists of the cell body, dendrites and an axon. The area where the axon diverges from the cell body is called the axon hillock and axon terminals are in the other end of the axon. These parts have different tasks in signal transferring. The cell body and dendrites are the input zone - they receive chemical signals and act upon them. The axon hillock is the trigger zone - that is where the action potential is generated if the signal is strong enough. The axon itself works as a conducting zone transporting the action potential to the terminals, that act as the output zone. [12]

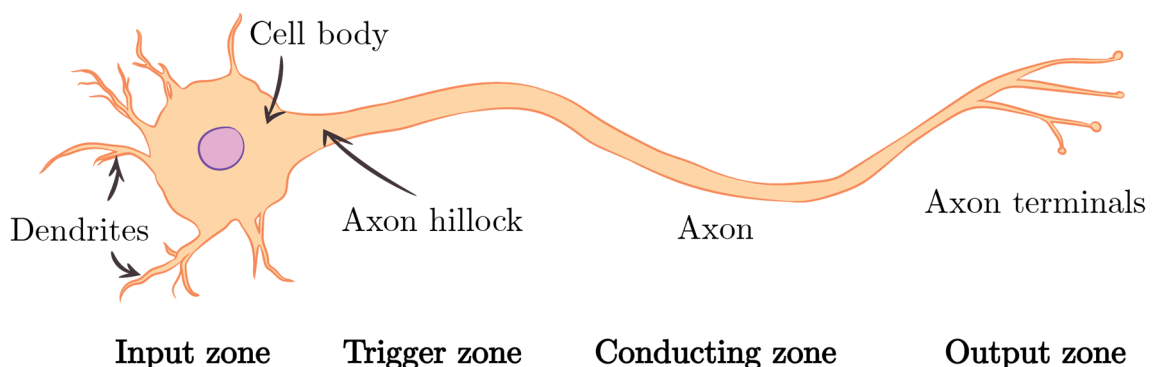


Figure 2: A Motor Neuron. Adapted from [12]

Almost all motor neurons (excluding those that innervate head muscles) are located in the spinal cord, from where their axons reach out all the way to the muscles they innervate. [12] The muscle fibers innervated by the same motor neuron comprise a muscle unit. A motor unit, on the other hand, includes both the motor neuron and the muscle unit. The motor unit action potential discharged from the spinal cord is called neural drive, while the muscle fiber action potential is referred to as muscle activation. The latter is recorded by electromyography, or EMG. [14]

To summarize, the signal path from brain to the muscle is illustrated in Figure 3. An activation signal is created in the brain from where it travels through the nervous system along a motor neuron to the axon terminals. When the signal reaches the neuromuscular junction, acetylcholine is released to the gap between the

terminals and the muscle fiber membrane. This excites the membrane and generates a potential gradient in the muscle fiber. This causes an inward flux of current, an intracellular action potential (IAP), or a depolarization zone. The depolarization zone, that is a few millimeters long, then starts to propagate from the junction, towards the tendons along the muscle fibers and the sarcolemma (the outer muscle fiber membrane) engaging contractile proteins, finally disappearing at the tendons. The higher the frequency of these signals, the more activated the muscle is. These changes in electric potential can be measured via electrodes placed on the skin surface above the measured muscle or inserted in the muscle. These methods are called surface and needle EMG respectively. [14] Textile electrodes are surface electrodes, and therefore needle EMG is not discussed in this thesis. The measured EMG signal is the sum of all action potentials discharging in the muscle fibers in the measured area, which is affected by the electrode location and size [14].

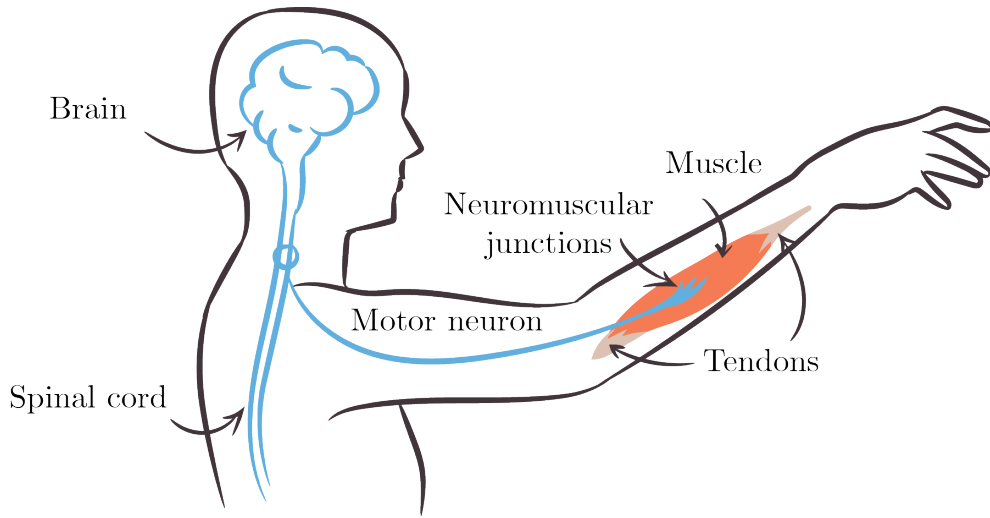


Figure 3: Signal path from brain to the muscle.

## 2.2 Electrodes as Transducers

Electrodes are an interface between the human body and the measurement device. They are transducers transforming ionic current of the human body into electric current. In theory, there are two kinds of electrodes: polarized and non-polarizable. Polarized electrodes work like capacitors – all the currents are displacement currents and no charge is transferred between the skin and the electrodes. In non-polarizable electrodes the oxidation is continuous and the current keeps flowing. However, in practice the electrodes are not completely one or the other, but a combination. [15] Most commonly used surface EMG sensors are made out of silver alloy due to their simple and cheap production and good electro-mechanical and antibacterial properties. Equation [1] describes the chemical reaction between a silver electrode and an electrolyte [16].



Silver is a metal from the noble end (+0.80 V half-cell potential [16]), which makes the electrodes prominently polarized. Still, they also have a resistive component and their impedance does not go to infinity at low frequencies. The electrode-electrolyte interface can then be modeled with the following circuit (Figure 4):

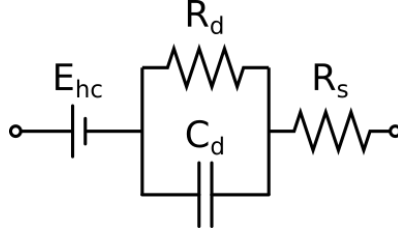


Figure 4: An equivalent circuit for the electrode-electrolyte interface. [15]

In Figure 4,  $E_{hc}$  is the half-cell potential of the electrode metal (silver in this case),  $C_d$  and  $R_d$  form the electrode impedance caused by the polarized ions and the chemical reactions on the metal surface, and  $R_s$  is the electrolyte resistance. [15]

Large impedance attenuates the signal and applies noise to low frequencies [17]. Part of this impedance is a property of the material and part of it is affected by the environmental factors such as humidity, temperature and the quality of the electrode-skin contact. For example, body hair and the amount of pressure the electrodes apply to the skin affect the contact area: more conductive fibers touch the skin with less hair and when pressure is applied to the electrode.

### 2.3 Conductive Textiles In Biosensing

Many different materials have been used for making textiles conductive, for example copper, stainless steel, silver, gold, nickel, conductive polymers and carbon black. [18]. Some applications of conductive textiles include stealth technology, camouflage [19], electromagnetic interference (EMI) protection, heating elements and signal transducers [20]. Silver is widely used in clinical applications due to its antimicrobial effects. Silver ionizes in the presence of water and the ions interact with bacterial and fungal cell membranes. Therefore, incorporating silver in the biosensing garments reduces the risk of infection and increases personal hygiene. [21]

### 2.4 Gesture Recognition

Gestures are body movements that convey information [22]. Many studies claim that gesture recognition (classification of such movements by analyzing recorded data) can be used for enhancing the HCI, or in other words, that gesture based communication with a robot or computer is more natural, realistic and immersive [23][24]. Gesture recognition methods can be divided into two groups: the vision based methods that extract features from image footage and the non-vision based that process data gathered by sensors. [25] All electrodes including the EMG measurement sleeves studied in this thesis fall under the latter category.

The proposed applications for gesture recognition include virtual reality (VR) and augmented reality (AR) interactions [24], sign language interpretation, robotics and telepresence [25]. Several studies have suggested doing gesture recognition from EMG data to control active prostheses [26][27][28]. Prostheses control is a demanding field of application in terms of reliability as unintended movements caused by incorrect classification are very frustrating for the user in every day life [29]. Furthering this line of research also acts as motivation for this thesis.



## 3 Design Process

The previous chapter is a theoretical view in electromyography. This chapter presents the practical choices of materials and methods made during the design process. A number of test samples were produced while designing the three prototypes that were used in the final measurements. Section 3.1 explains the purpose of each sample and weighs the pros and cons behind each design decision. Section 3.2 introduces a smaller scale test sleeve intended for impedance spectroscopy and frequency response measurements. It features the final electrode design but contains just one electrode pair made of each material. Finally, Section 3.3 presents the final eight channel electrode sleeve design intended for the actual EMG measurements.

### 3.1 Materials and Manufacturing Methods

#### 3.1.1 Base Garment

The first task in the design process was to choose the base that the electrodes would be sewn on. The end goal was to create an 8-channel electrode array that could be connected to OT Bioelettronica Sessantaquattro measurement device for acquiring the EMG. Taken into account that the electrode array should be equidistantly spread around the forearm and that the subjects will have varying forearm circumferences, it was necessary to ensure the garment material is elastic.

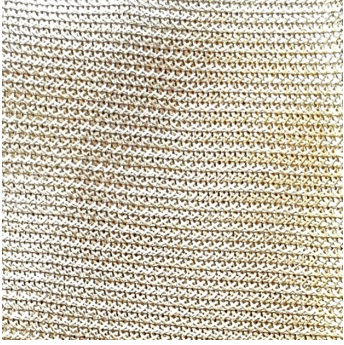

Another important requirement was to establish a good connection between the skin and the electrodes. This means that the electrodes should not have room to move around and the garment should mold to the shape of each test subject's forearm. For this reason, the garment should also have a tight fit. Furthermore, the garment should not be conductive as that would short-circuit the electrodes.

A sports compression sleeve was chosen as the base and the electrodes were sewn the reverse side of it. A product made by Compressionz was selected mainly because it was relatively inexpensive and readily available in sufficient quantities. It is elastic, not very thick and non conductive.

#### 3.1.2 Conductive Fabrics

After choosing the base for the electrodes, the conductive materials for the electrodes were acquired. Statex [30], a Germany based textile manufacturer provides a wide range of conductive fabrics. They had several suggestions specifically for biosensing purposes. Table 1 lists the two most conductive of the recommended fabrics called Bremen and Balingen and their key features. The main difference between these two is that Balingen is knitted and thus elastic while Bremen that is woven does not stretch. Although the sheet resistance of Balingen is twice that of Bremen, they are both very conductive. Balingen is also thicker and heavier than Bremen. One prototype was constructed using each of these materials.

Table 1: Used fabrics and their properties. Values for the conductive threads are taken from technical data sheets provided by Statex.

	Shieldex Balingen	Shieldex Bremen RS
		
Material	Silver plated knitted polyamide fabric	Silver plated woven polyamide fabric
Sheet resistance	$< 0.6\Omega/\square$	$< 0.3\Omega/\square$
Thickness	0.26 mm $\pm 10\%$	0.090 mm $\pm 12\%$
Weight	62g/m <sup>2</sup> $\pm 10\%$	43g/m <sup>2</sup> $\pm 10\%$

### 3.1.3 Conductive Threads

As a comparison for the two types of fabric electrodes, a third electrode sleeve prototype was made embroidering directly on the sleeve with a conductive thread. Table 2 lists all the threads used in the design process. In addition to the non-conductive polyester thread used for attaching parts together, the table lists the two most suitable conductive threads for embroidering purposes: Madeira HC12 and Madeira HC40 by Statex [30]. Later in the thesis, they will be referred to as HC12 and HC40. The main difference between the two is that HC12 is thicker and more conductive.

### 3.1.4 Stitching and Embroidering

The main tool in the prototype manufacturing process was a sewing machine (Toyota Oekaki50, [31]). Usually, a sewing machine is used for attaching two or more layers of fabric together using two threads: the upper and the bottom thread. Figure 5 depicts the machine and the routes of the upper and the bottom thread. As can be observed, the upper thread goes through many turns before reaching the needle eye.

Table 2: Used threads and their properties. Values from technical datasheets provided by Statex.

Name	Material	Resistivity
Coats Duet TK100 100m	100% polyester corespun thread	non-conductive
Madeira HC 12 (235 dtex)	Silver plated polyamide yarn	$< 100\Omega/m$
Madeira HC 40 (117 dtex)	Silver plated polyamide yarn	$< 300\Omega/m$

It was noted that the surface of the upper thread could be damaged rubbing against sewing machine parts, as the conductive threads are in fact conductive due to a silver coating. This concern was relieved in the embroidery experiments described later in this section.

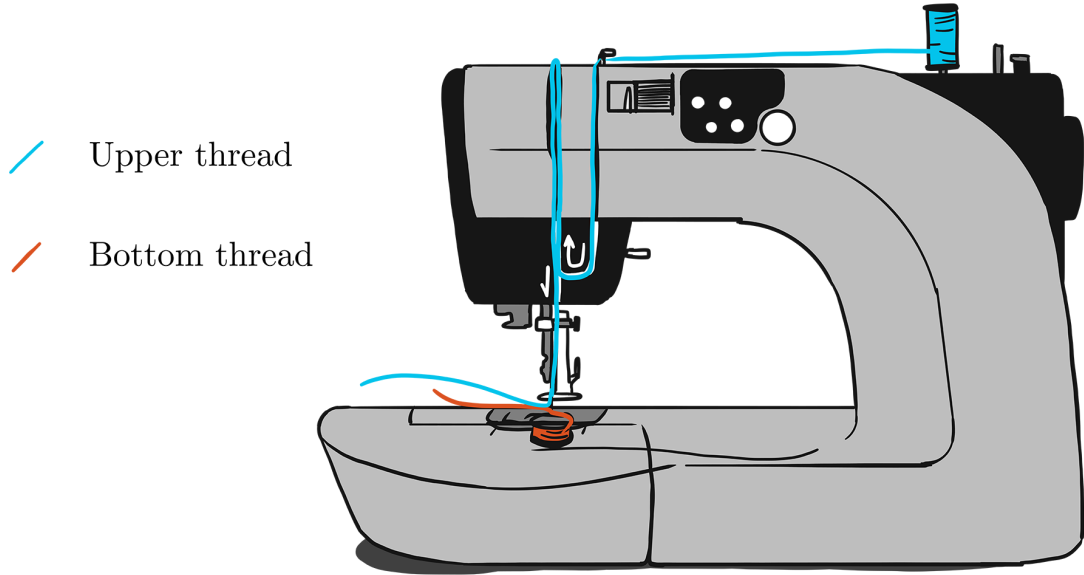


Figure 5: A technical drawing of Toyota Oekaki sewing machine and the routing of the upper and bottom threads.

Thread tension is one of the settings in a sewing machine. Figure 6 illustrates the resulting problems when the tuning is not right. This problem manifested in the embroidery experiments, as the conductive threads were much thicker and more rigid than a normal polyester thread resisting the movement through the sewing machine and causing tension.

There are several types of stitches a sewing machine can perform intended for different uses. The stitch used for attaching the electrodes to the sleeve needs to prevent the conductive fabric square from unraveling and it has to be able to stretch along with the sleeve. A traditional option for this purpose would be zigzag stitch. Figure 7 presents the three tested options for stitching a square electrode on a fabric.

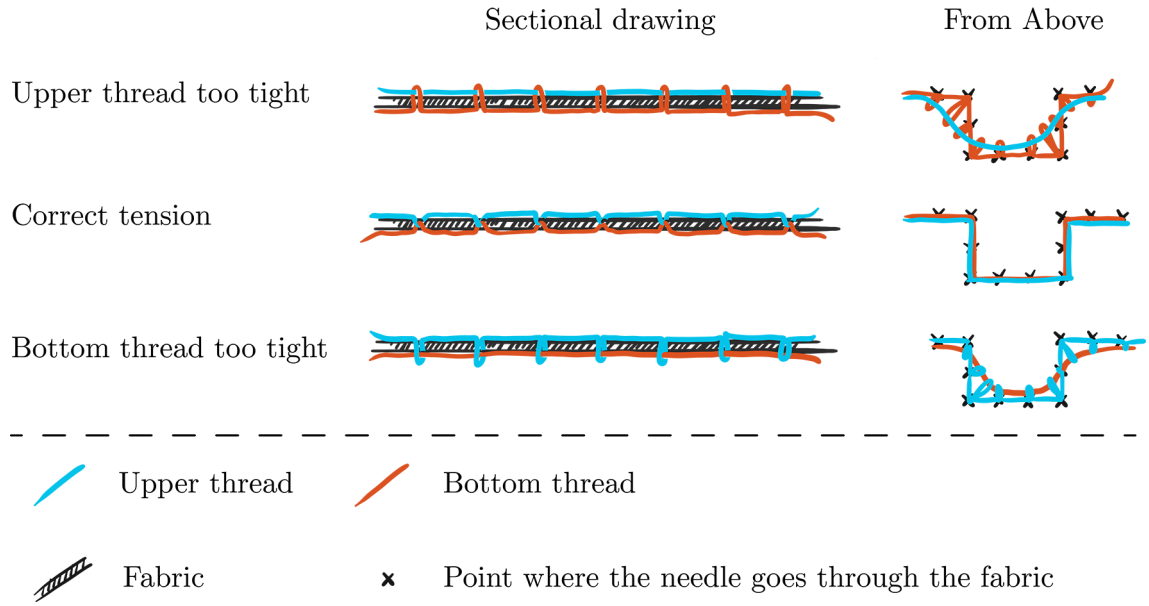


Figure 6: A sectional drawing of a straight stitch and a drawing from above of a stitch changing directions in different thread tension situations. This illustrates the effect of thread tension settings.

Zigzag stitch with short stitch length in Figure 7a prevents unraveling very efficiently but covers a large part of the electrode area and is extremely slow to apply. Longer stitch in Figure 7b leaves more area open for skin contact, but the best stitch in this regard and the final choice was the overcasting stitch presented in Figure 7c.

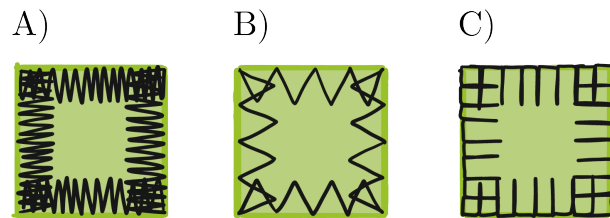










Figure 7: The tested stitch choices for attaching the fabric electrodes to the sleeve: A) short zigzag stitch, B) long zigzag stitch, and C) overcast stitch.

In addition to the basic stitches found in most sewing machines, Toyota Oekaki50 has a freehand embroidering setting called Oekaki that was used for making the embroidered electrodes. The stitch width can be adjusted from zero to five millimeters. A wide stitch similar to zigzag stitch could have covered more area while embroidering. However, the rigidity of the conductive threads lead to the thread breaking and warped the fabric preventing the creation of accurate electrode shapes, such as circles and rectangles. For this reason the embroidered electrodes were sewn on using the Oekaki setting with zero stitch width, which means a straight stitch. The electrode was implemented by filling in a 10 mm by 10 mm area with a fine grid.

An experiment was conducted to determine the best combination of the top and

bottom threads. Table 3 presents the results of the experiment. Using conductive thread as both the upper and the lower thread are not included, because the threads kept braking and the fabric got repeatedly stuck in the sewing machine thus making it impossible to finish the electrodes. The assumption was that using the conductive thread as the upper thread would rub the conductive coating off and increase the electrode resistance. However, when measuring the resistance over the electrode diameter there was no significant difference between using the conductive thread as the upper or the bottom thread. Furthermore, using it as the bottom thread was harder to control and resulted in warping the fabric ruling it out as an option. HC12 was chosen to be used in the sleeve prototype as it had lower resistance than HC40 and it was still manageable to work with. The results of the embroidering experiment were clearly affected by the very elastic sleeve material. Thicker and less elastic materials could lead to a different outcome.

Table 3: Behavior of different thread combinations on the sleeve fabric

Upper thread	Bottom thread	Right side	The reverse	Side-to-side resistance ( $\Omega$ )
HC 12	Coats Duet			1.5–2.5
Coats Duet	HC 12			1.5–3
HC 40	Coats Duet			3–6
Coats Duet	HC 40			3–5



### 3.1.5 Electrode Dimensions

Other properties related to the electrodes are the shape, size and interelectrode distance. The electrode size and interelectrode distance were decided solely on the SENIAM recommendations [32]. The SENIAM project, that is short for "Surface Electromyography for the Non-Invasive Assessment of Muscles project", is a European concerted action in the Biomedical Health and Research Program, or BIOMED II, of the European Union. The recommendation is to use circular electrodes with a 10 mm diameter and 20 mm interelectrode distance, which is measured between the center points of two adjacent electrodes. The choice of shape was not as simple: it significantly affected the difficulty and time-efficiency of the manufacturing process. A simple experiment was conducted to assess the effect.

Figure 8 presents the results of experimenting with different electrode shapes on both Balingen and Bremen fabric. Samples A and B in Figures 8a and 8b are made of Balingen and the samples C and D in Figures 8c and 8d are made of Bremen. A circular shape was investigated in samples A and C and a rectangular shape in samples B and D. Sewing on an elastic fabric posed some challenges. The round electrodes (samples A and C) were slower to sew on and the fabric got wrinkled more easily. Using rectangular electrode shape (samples B and D) was substantially more efficient and did not distort the fabric as much. In the final prototypes, the amount of electrodes that had to be sewn on was large, so an efficient work flow was crucial, and for that reason the rectangular shape was chosen.

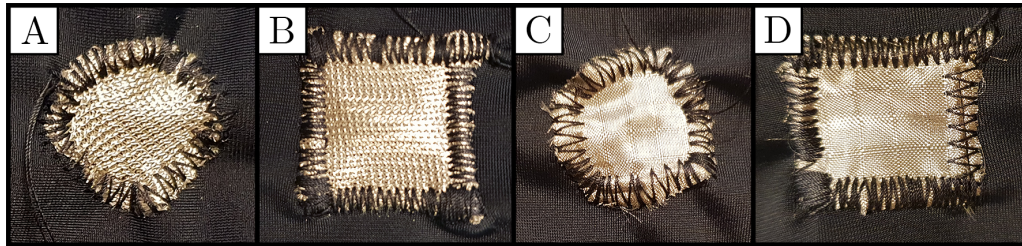


Figure 8: Fabric electrode shapes

## 3.2 Single electrode pairs

Before constructing the full electrode array, the electrical properties of a single bipolar electrode pair made of each material were measured. The impedance spectroscopy and frequency response measurements performed on this prototype are described in Sections 4.1 and 4.2 of Chapter 4.

Figure 9 presents the blueprint of the design. There are three pairs of electrodes equally spaced around the sleeve. The electrodes are 15 mm by 15 mm squares with 20 mm interelectrode distance. Figure 10 presents the finished electrodes. A reference electrode is placed in the wrist area an equal distance from each pair. It was essential that all three electrode pairs had as similar environmental parameters as possible to achieve comparable results. For example, the skin-electrode impedance could be affected by the pressure applied on the electrodes [33]. Placing all three electrode

pairs on the same sleeve eliminates any pressure differences and with this symmetrical design the electrical interference between the electrode pairs is minimal. Metallic snap buttons were hand sewn on the other side of the electrodes with conductive thread. The only asymmetrical feature in the sleeve is the zipper that allows the sleeve to be put on an arm.

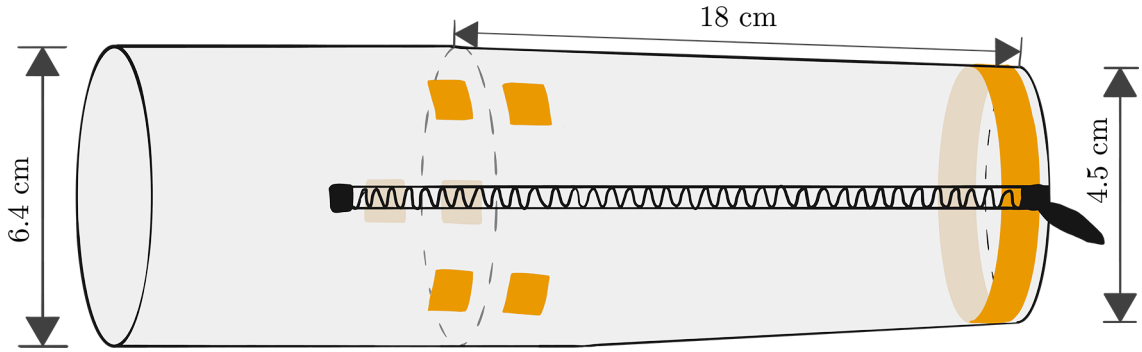


Figure 9: Technical drawing illustrating the electrode arrangement on the first prototype.

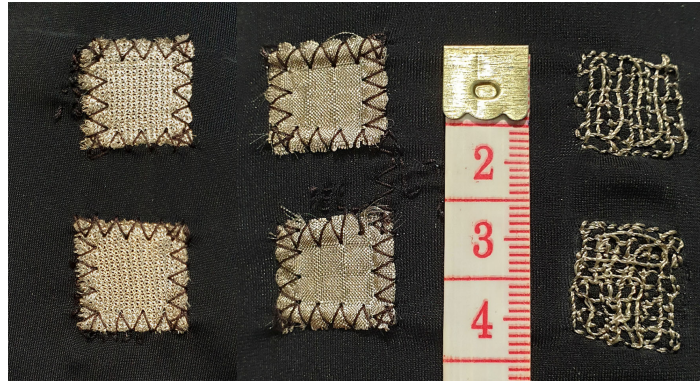


Figure 10: The electrodes on the first prototype. From left to right: Balingen, Bremen, HC12.

### 3.3 Electrode Array Sleeves

For the final EMG measurements, one sleeve dedicated for each of the three materials was constructed. Figure 11 presents the blueprint of the final design. The sleeve has 16 electrodes placed equidistantly in pairs to create 8 bipolar EMG input channels for the Sessantaquattro device to record. The electrodes are 10 mm by 10 mm rectangles with an interelectrode distance of 20 mm. As discussed in Section 2.3, the overcasting stitch covered the electrodes the least while providing a stretchy fastening to the sleeve.

In this final design, the reference electrode was separated to prevent the sleeve from becoming a volume conductor. One reference electrode bracelet was made for

each sleeve with the corresponding electrode material. Figure 12 presents the finished prototypes turned inside out exposing the electrodes. Figure 13 shows one of the sleeves worn on the arm and in this picture also the snap buttons used for connecting to the measurement device are visible. The snap buttons were hand sewn on the other side of the electrodes with conductive thread.

The tight space inside the sleeve posed some reaching difficulties with the sewing machine and Bremen fabric presented most difficulties with unraveling while the embroidering technique was the easiest to control.

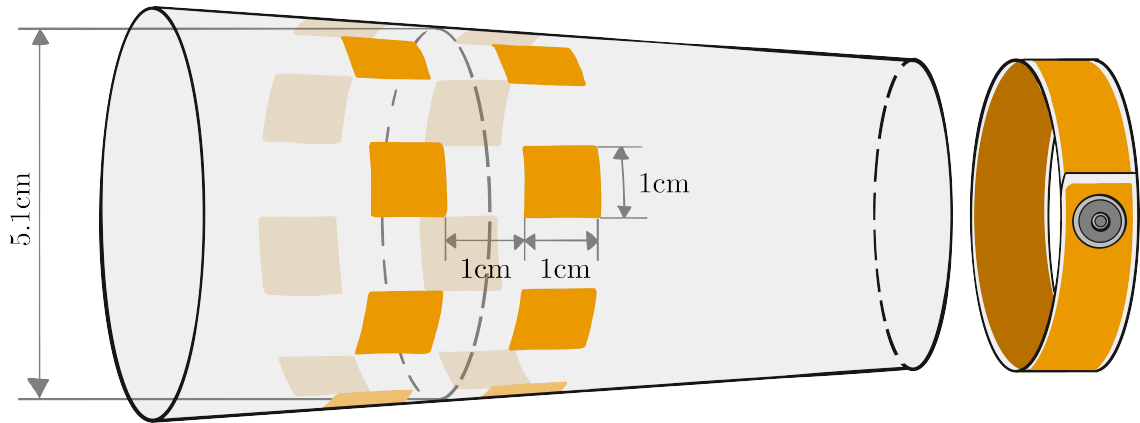


Figure 11: A technical drawing describing the structure of the final prototype. The interelectrode distance and electrode width and height is 1 cm and the diameter of the sleeve measured from between the electrode pairs when not stretched is 5.1 cm. The conductive fabric parts are highlighted with orange color.





Figure 12: Compression sleeves with 8 equally spaced electrode pairs and their reference electrode bracelets.



Figure 13: Electrode array sleeve worn on the right arm.

## 4 Validation

Chapter 3 explained the design process that produced four prototype sleeves – one that includes one bipolar electrode pair made of each of the three materials that were chosen to be investigated and three sleeves with eight bipolar channels, one sleeve dedicated to each of the three materials. This chapter focuses on analysing their electrical properties and determining how well they perform in EMG measurements and gesture recognition. They were compared to the self-adhesive silver/silver chloride wet electrodes (Ambu Neuroline 720, Denmark [34], later referred to as Ambu720) that have a contact area of 30 mm by 22 mm. Section 4.1 contains the impedance spectroscopy measurements and Section 4.2 measures the frequency response experimenting with different input signals. These measurements are performed on the one-channel prototype. Section 4.3 includes the EMG measurements performed on people with the eight-channel prototypes. The section is divided into three subsections: 4.3.1 establishing signal baseline, 4.3.2 assessing the maximal voluntary contraction signals, and 4.3.3 the gesture recognition using machine learning. Signal baseline provides information about the DC offset and the noise in the signal, the MVC measurement is more of a qualitative check and the gesture recognition results are used to assess whether the textile electrodes could replace the conventional electrodes in prostheses control. Each section goes through the respective measurement methods, results and discussion.

### 4.1 Impedance Spectroscopy

The electrode–skin contact impedance is one of the parameters that affect the signal quality of EMG measurements. As discussed in Section 2.2, high electrode impedance causes low frequency noise and signal attenuation. Impedance spectroscopy was performed on the prototype described in Section 3.2 to determine the impedance characteristics of the materials under study.

#### 4.1.1 Methods

The measurement setup was adapted from a study by Gruetzmann [33]. Similarly to [33], one electrode pair was measured at a time and the electrodes were placed on the left forearm of the test subject. The selected spot was on top of flexor carpi radialis, a muscle used for flexing the wrist (see Figure 14). Between the measurements, the sleeve was rotated and the next pair was carefully placed on the same location as the previous to minimize the variation between the measurement conditions. First, the measurements were performed with a dry sleeve, after which the sleeve was wet slightly with tap water and the measurements were repeated. The self-compression of the sleeve was the only pressure applied on the electrodes.

The electrodes were connected to an impedance analyzer (Keysight E4990A, USA) according to Figure 14. The impedance was measured over two electrodes, that is the impedance of two electrode-skin impedances in series. The frequency sweep was performed from 60 Hz to 100 kHz. The measurement performed in [33]

was performed between 30 Hz and 100 kHz. Although according to specifications E4990A is capable of measuring from 20 Hz on, the results below 60 Hz were not reliable. The acquisition was set to "precise" setting and the results are the average of five consecutive sweeps.

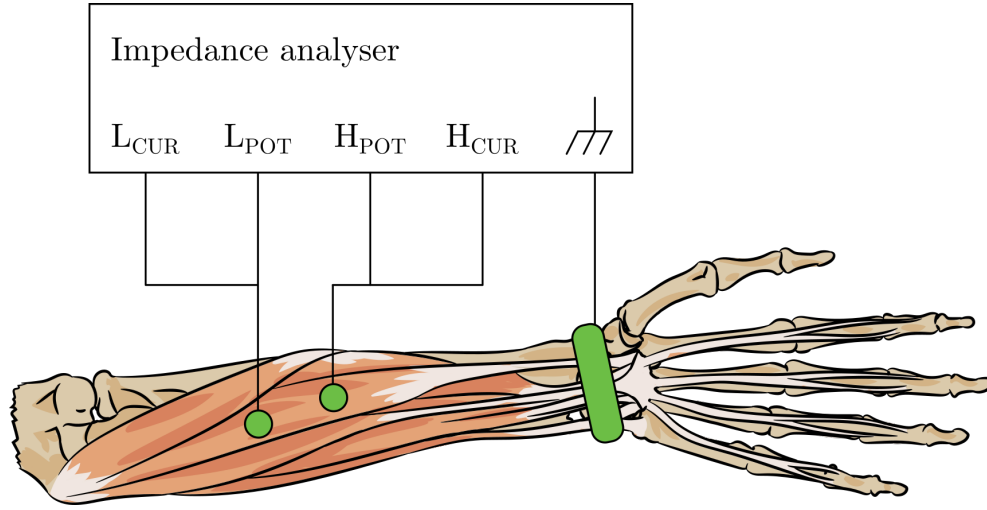


Figure 14: The schematic diagram of the impedance spectroscopy measurement setup showing the electrode locations on the left forearm. Reference electrode wrist band is connected to the chassis ground. The impedance analyser used is Keysight E4990A.

#### 4.1.2 Results And Discussion

Figure 15 represents the magnitude and the phase of two electrode-skin impedances in series. The difference between electrode impedance before and after wetting is significant. Surprisingly, the wet textile electrodes have even lower impedance at lower frequencies than Ambu720. In this regard, the results suggest that textile electrodes are a strong alternative for the conventional wet gel electrodes.

However, results also show that while the impedance of the wet Balingen electrodes is the smallest, the impedance of dry Balingen electrodes is the largest. The impedance changed the most between dry and wet out of all the textile electrodes, which suggests that it reacts the most to the changes in moisture. This could lead to Balingen experiencing the most changes in signal noise when the electrodes dry.

Ambu720 impedance curve is straight which means that it has a definite power relationship to frequency ( $f^{-1}$ ), whereas the wet textile electrode impedances are quite constant at lower frequencies and start to have the same power relationship at higher frequencies. The dry textile electrodes, on the other hand, also have a consistent power relationship. This means that the impedance-frequency relationship changes somewhat depending on how wet the textile electrodes are. This leads to changes in the attenuation of lower frequencies compared to higher frequencies, which could mean that not only the amplitude, but also the shape of the EMG signal spectrum changes according to the wetness of the electrodes, which could be a problem in gesture recognition applications.

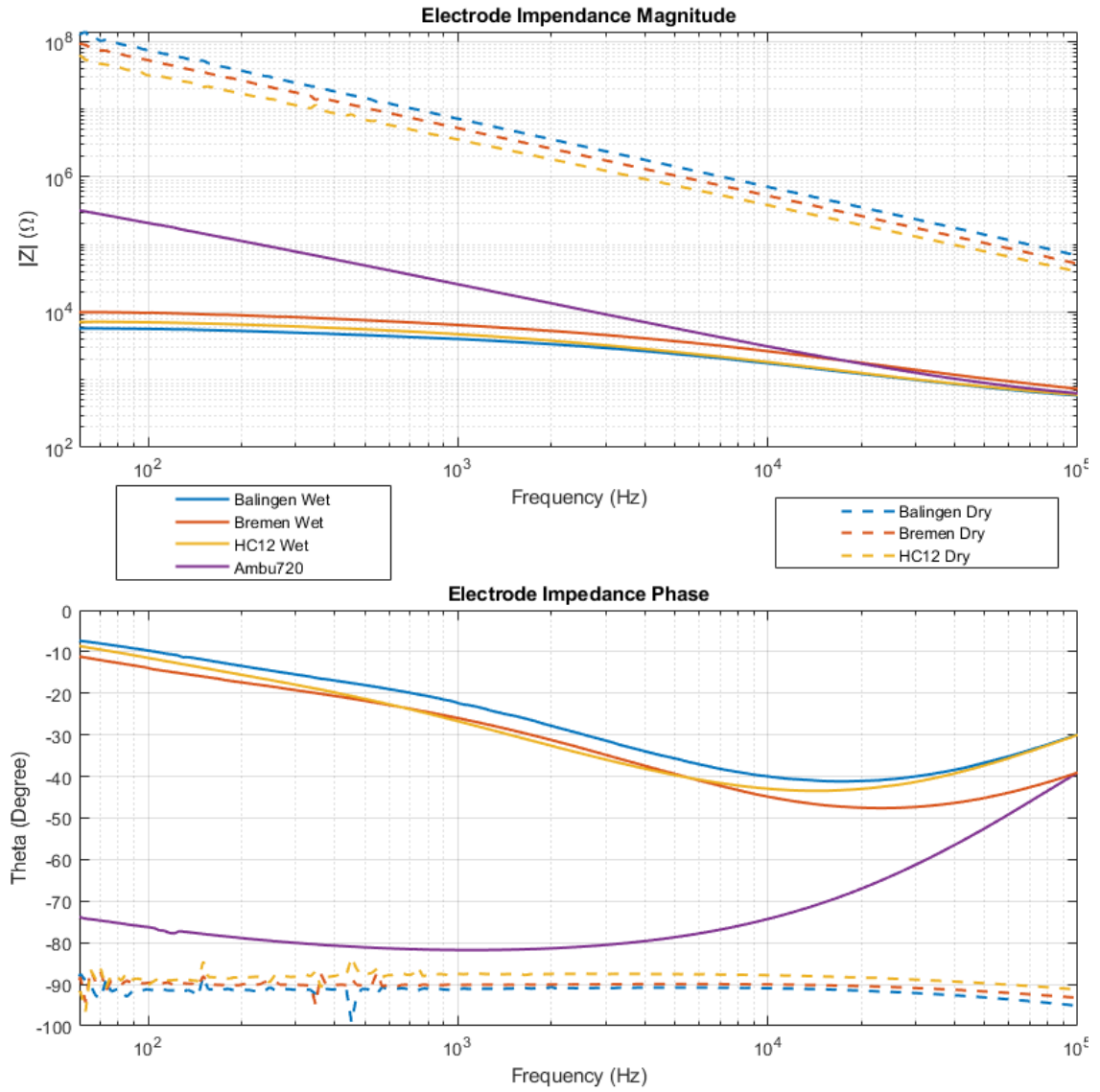


Figure 15: The electrode impedance magnitude and phase results of the dry textile electrodes (dashed lines), textile electrodes that have been doused with water (solid blue, red and yellow lines) and Ambu720 (purple line). Surprisingly, the wet textile electrodes had lower impedance than Ambu720.

## 4.2 Frequency Response

### 4.2.1 Methods

The signal transferring characteristics at different frequencies were further investigated through series of frequency response measurements. The measurements were performed on the prototype that is described in Section 3.2. The input signals were sinusoidal and square waves with 10, 100, 1000 and 10000 Hz frequencies. The input signals were generated with a function generator (Thurlby Thandar Instruments TG120, United Kingdom).

The input signal was fed to the electrode on the inside of the sleeve and was measured from the other side according to Figure 16. To simulate the physical conditions, such as pressure applied on the electrode when measuring on a human arm, the sleeve was placed upon a test bench that consists of a plastic dome that has been embedded with metal contacts (see Figure 17). The contacts are used for feeding the generated signal to the measured electrodes. Only one of the contacts was in use during this measurement.

The generated and the measured signals were connected to a USB audio interface (Steinberg UR22mkII, Germany) and were recorded as a stereo audio signal with 192 kHz sampling rate and 24-bit resolution using an audio software (Audacity) on a computer. The setup was calibrated by adjusting the levels while feeding the generated signal to both channels.

The signal was recorded for 10 seconds in other cases, but 20 seconds in the case of 10 Hz signals to gather enough pulses for more reliable results. The first and last second were omitted to minimize the effect of environmental factors when starting and stopping the recording. The data was analysed by fast Fourier transform (FFT).

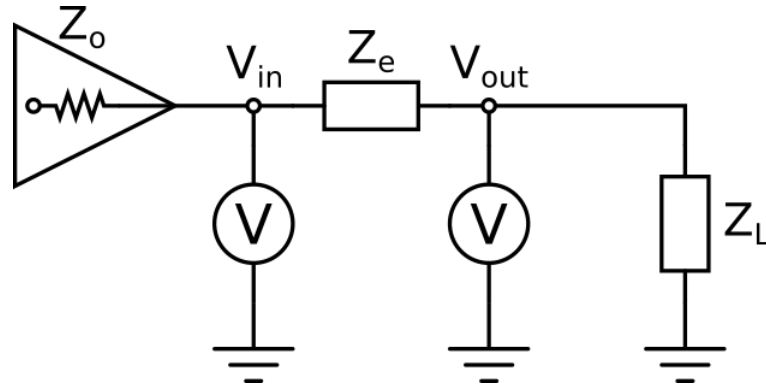


Figure 16: Electrode frequency response measurement setup.  $Z_e$  is the impedance of the measured electrode. The function generator has a  $50\ \Omega$  output impedance ( $Z_o$ ). The load resistance ( $Z_L$ ) is also  $50\ \Omega$ . The input signal ( $V_{in}$ ) and the output signal ( $V_{out}$ ) were recorded as a stereo audio signal using a 24-bit USB audio interface with 192 kHz sampling rate (Steinberg UR22mkII) and a recording software (Audacity, [35]) on a computer.

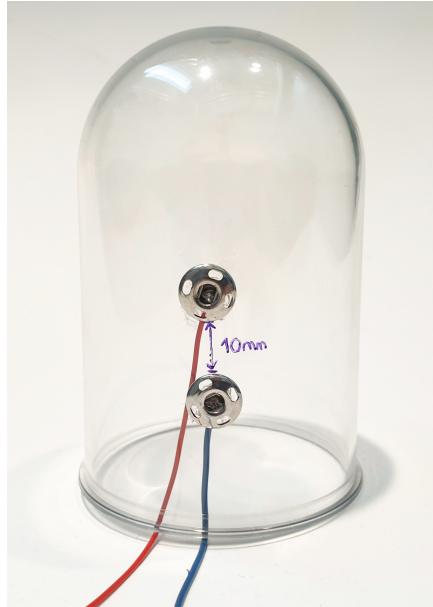


Figure 17: Testbench for measuring the electrodes. It consists of a non-conducting plastic dome with embedded conductive pads for feeding the test signals into the prototype electrodes.

#### 4.2.2 Results And Discussion

Figure 18 presents the Fourier transformation for the sine wave input signals and Figure 19 for the square wave input signals. There are no significant harmonic frequency components in the sine wave measurements, so the graphs show the main frequency component in more detail. The results show no frequency shift or spectral broadening in the signal – only attenuation, which can be countered with appropriate amplification and signal processing [17].

Figure 20 summarizes the amount of attenuation in each case. The results are not very conclusive. There is no clear ranking between the different materials nor are the results consistent between the shape of the input signal. Balingen seems to perform exceptionally badly with 10 Hz sine wave, but otherwise on average HC12 performs marginally worse than others.



Sine wave measurements in frequency domain

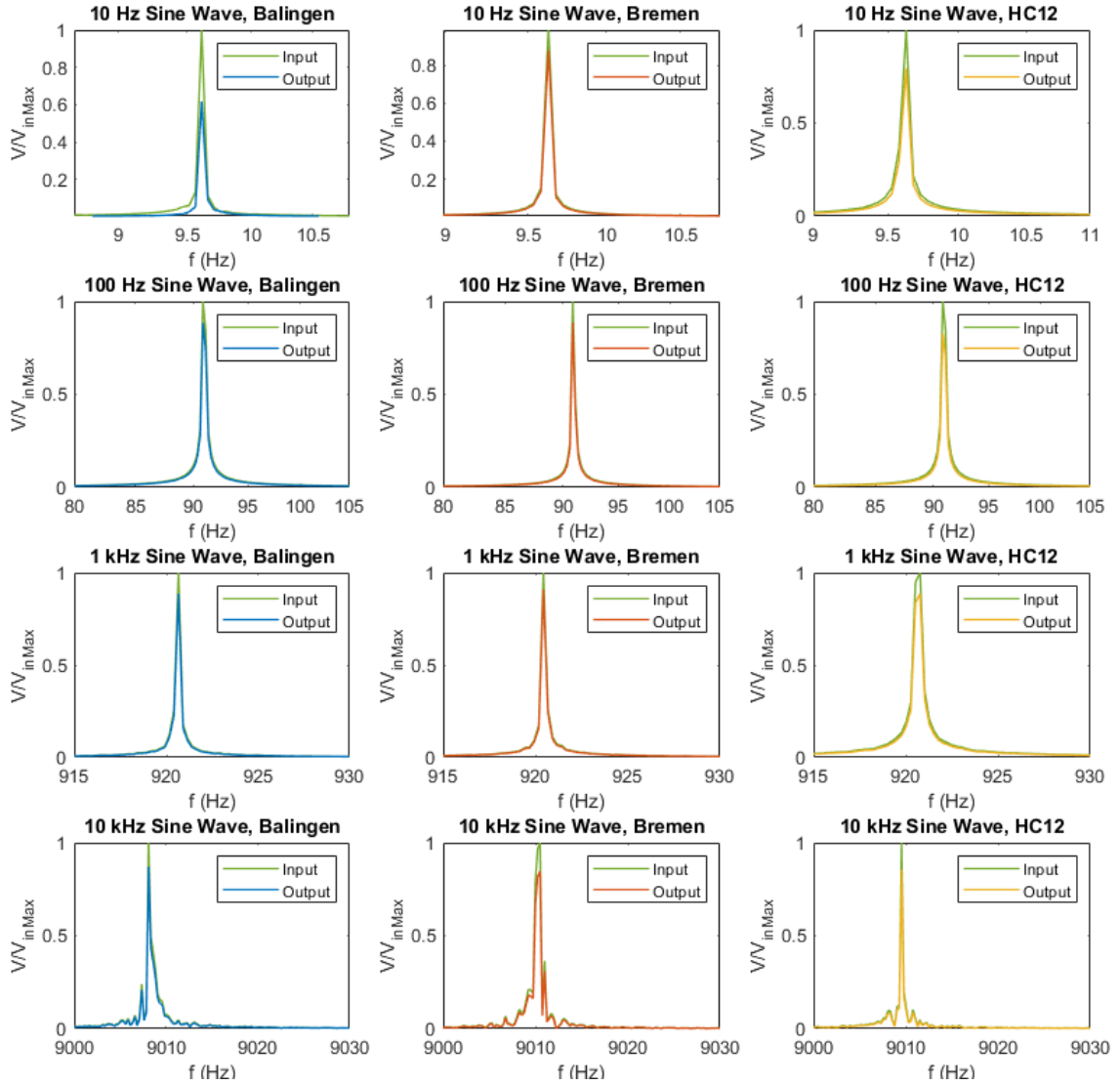


Figure 18: The result of FFT for sine wave input signals. There is no noticeable change in the shape of the main frequency components – only attenuation. The generated 10 kHz signal was lower quality than other signals, but the response still follows the same shape.

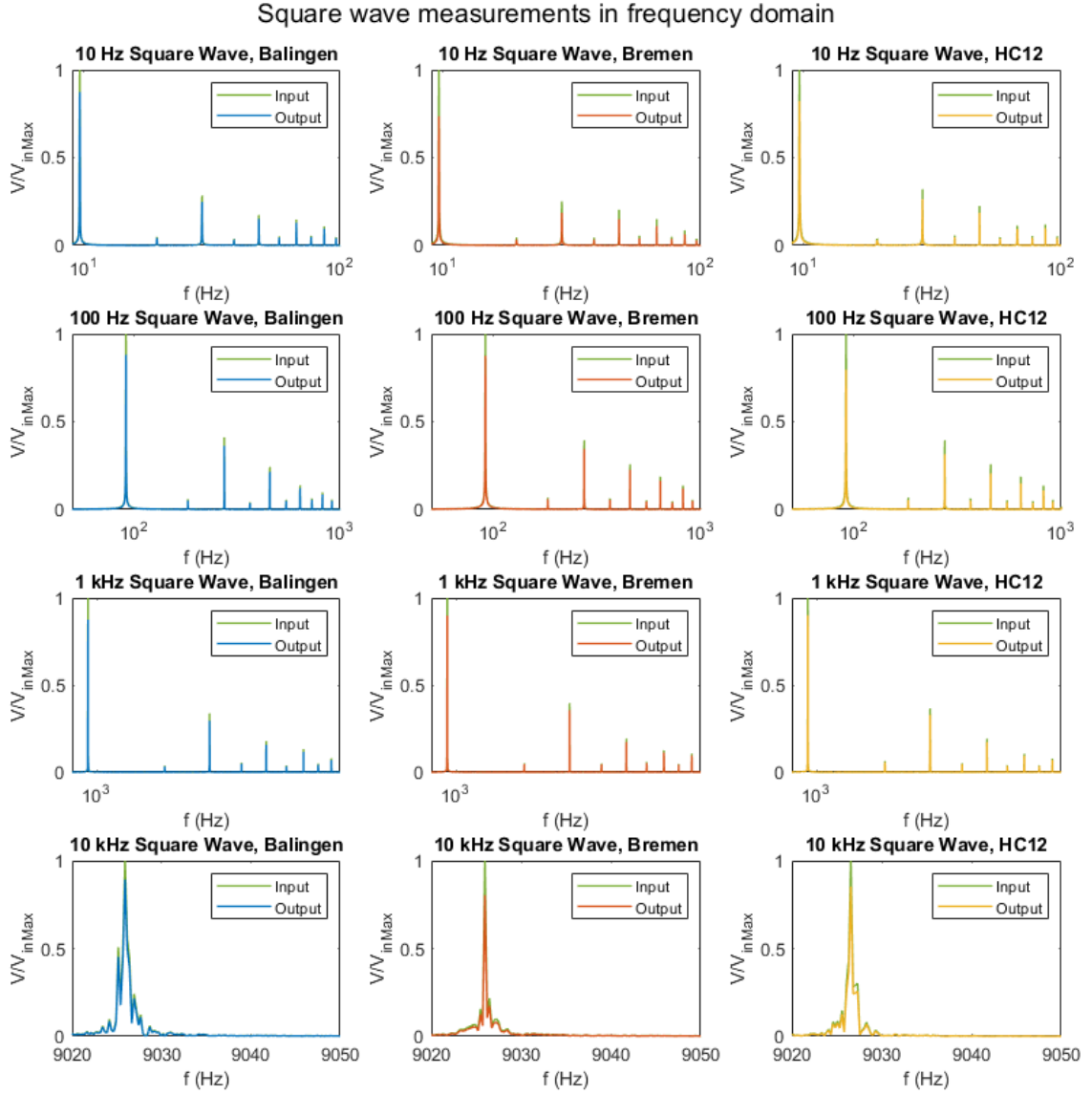


Figure 19: The result of FFT for square wave input signals. The only difference between the input and output signals seems to be attenuation. Differing from the sine wave, the square wave has several harmonic frequency components. The higher frequency components of the 10kHz square wave were not within the measurement range.



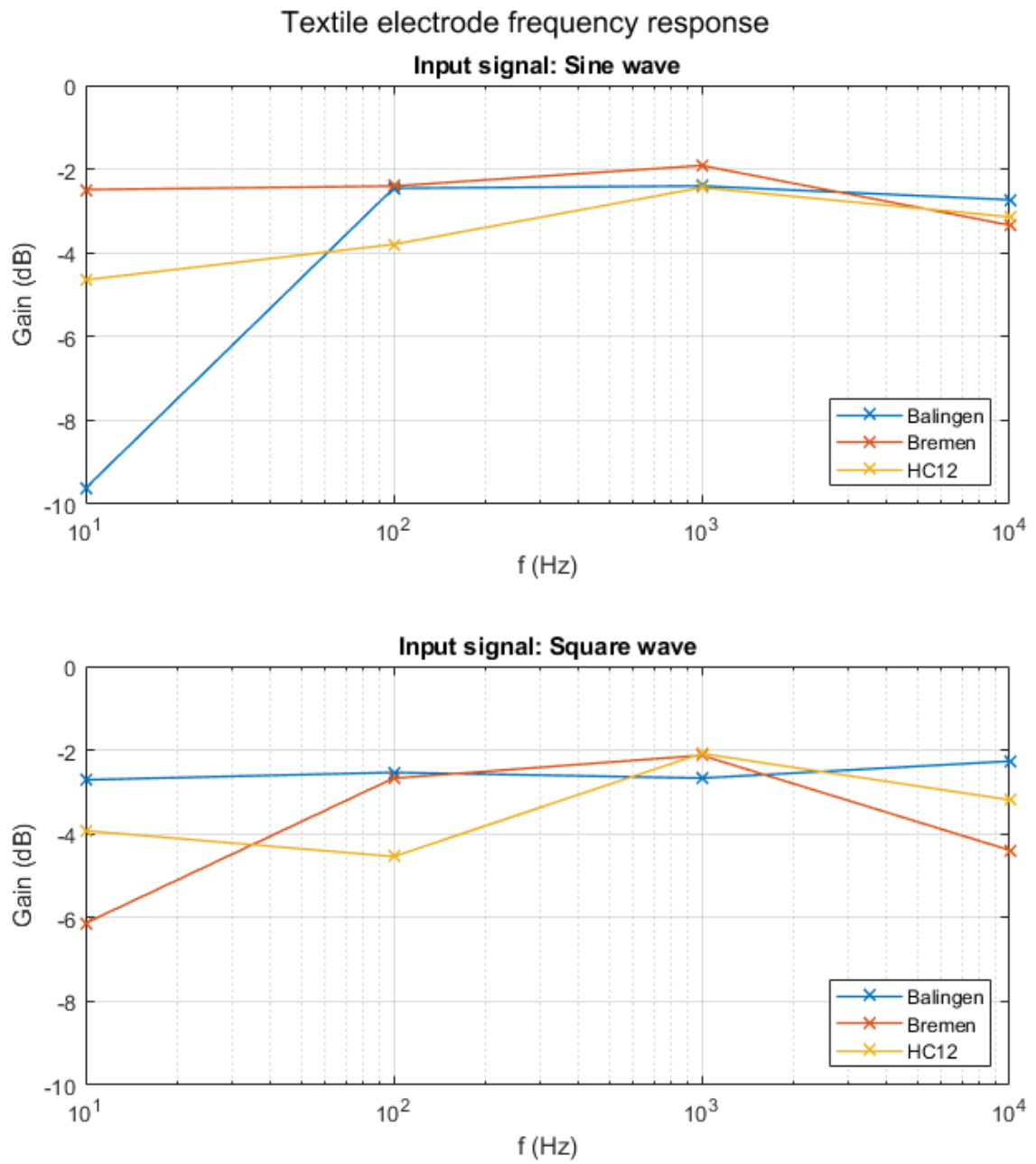


Figure 20: Summary of the gain of the main frequency component in each frequency response measurement. There is no significant difference between the different textiles.

### 4.3 EMG Acquisition Performance and Gesture Recognition

The eight-channel prototype sleeves described in Section 3.3 were tested on eight subjects (age  $28 \pm 3$  years, 6 males and 2 females). Three different EMG measurements were performed to establish several signal properties and the electrode array functionality in hand gesture recognition.

The electromyography measurements were conducted using an acquisition device (OT Bioelettronica Sessantaquattro, Italy) and software (OT Bioelettronica OT Biolab+, Italy). Figure 21 shows the measurement setup connected to a subject with the sleeve and with the Ambu720s. The acquisition device, placed on the table, has a WiFi connection to a computer running the acquisition software. The acquisition device was configured to measure 8 bipolar channels with a sampling frequency of 2 kHz. The channels have a 10 Hz high pass filter, a 500 Hz low pass filter and a gain of 256. The electrodes were placed on the subject's dominant hand, around the forearm muscle belly.

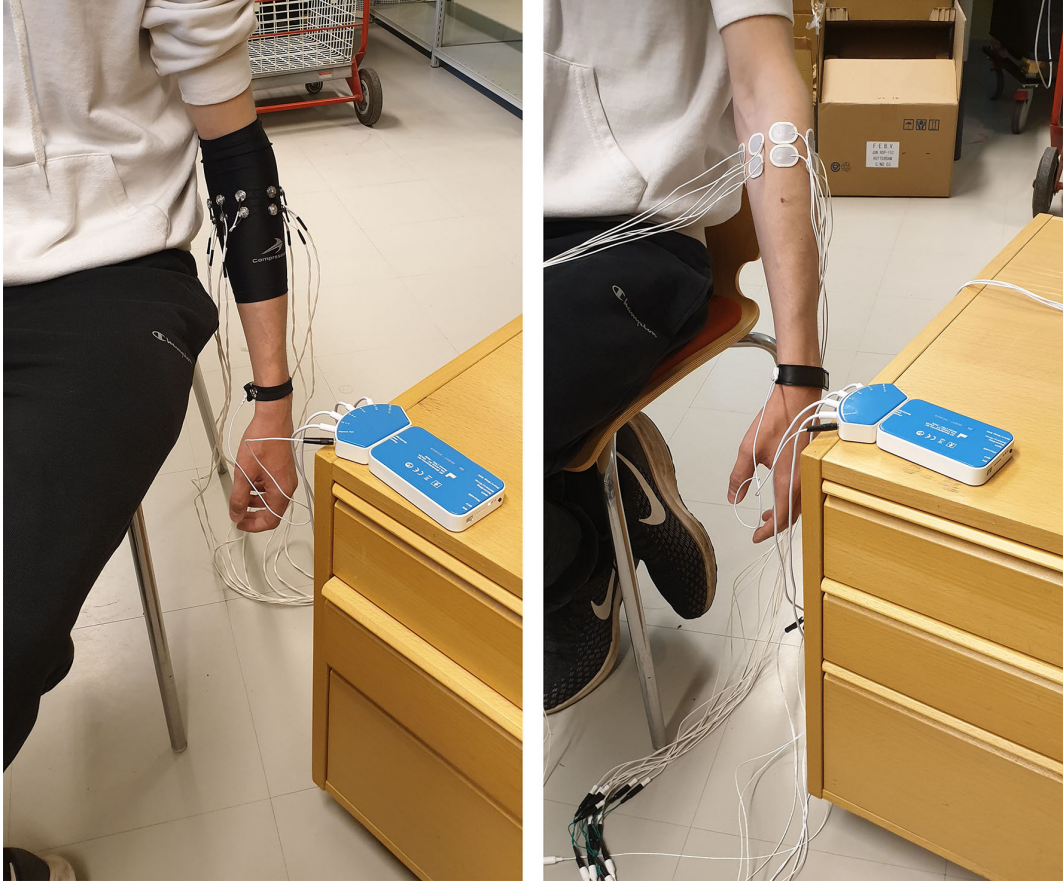


Figure 21: The electromyography measurement setup on a subject: one of the sleeves on the left and Ambu electrodes on the right.

The visual feedback feature of the acquisition software was used for standardizing the execution of the motions during both the maximum voluntary contraction (MVC)

measurement and the functionality test. Trapezoidal feedback was used as a visual guide for the subject to adjust the amount of contraction in a proportional way during the measurement. The height of an animated bar on the computer screen changed as a function of time (Figure 22), the lowest level corresponding a complete limb rest and the top of the shown profile cued the maximum desired level of contraction. The steady rising and falling edges encourage the subject to take their time switching between relaxation and contraction thus avoiding abrupt movements and motion artifacts in the data. The length of the plateau and the relaxation period differs between the measurements: the MVC's are shorter than the contractions performed in the functionality test but require more time to relax the muscles and recover before the next contraction.

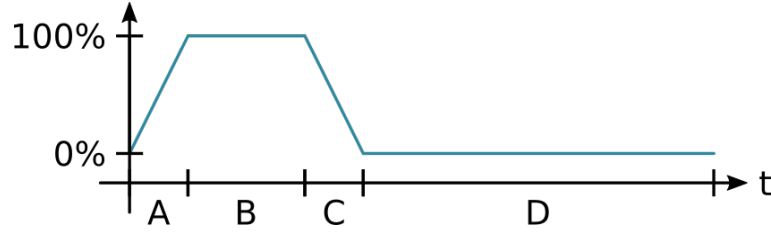


Figure 22: Trapezoidal feedback is a visual guide for the subject to time the contractions correctly. It comprises of the rising edge (A), the plateau (B), the falling edge (C) and the relaxation period (D). The graph illustrates the height of an animated bar on the computer screen as a function of time. The bar height corresponds to the amount of contraction that is required from the subject at a given time.

The measurement protocol consisted of four measurement steps for each subject. First, the baseline of the signal when the muscles are relaxed was acquired (Section 4.3.1). Then, the prototype's susceptibility to muscle movement due to external impacts was tested by repeating the first recording while tapping the forearm from different directions. Third, the maximum voluntary contractions (MVC) were recorded in the chosen 8 motions (Section 4.3.2). And finally, a longer EMG experiment was conducted where multiple samples of 8 motions and relaxed state were gathered. The data was used in data classification test to see how textile electrodes compare to wet gel electrodes in gesture recognition applications (Section 4.3.3).

#### 4.3.1 Signal baseline and resistance to interference

The signal baseline was examined with two twenty-second measurements on a relaxed arm. During the second measurement, the subject's forearm was tapped gently around the electrodes. Figure 23 compares the results across the different electrode setups and subjects. Each bar represents the average value across all channels measured on a single subject, the error bars being the standard deviation. Figure 23a presents the results without tapping and Figure 23b features the tapping. The results suggest that the DC-offset is very similar between all the electrode setups and stays close to 0 volts even with physical interference. The standard deviation, which translates to the noise that is picked up by the electrodes, is considerably larger in Ambu720s without tapping. However, introducing tapping increases noise in all the other setups consistently by an order of magnitude while the noise picked up by the Ambu720s remains lower. The results show, that HC12 electrodes are the least sensitive to noise in calm circumstances whereas Ambu720s deal better with physical interference.

#### 4.3.2 Maximum Voluntary Contraction

Maximum voluntary contraction measurements are used by researchers, physiotherapists and athletic trainers to study ergonomics and provide feedback [36]. Here, MVC is investigated to compare the strength of the signals measured with the different electrode setups and to visually inspect the signal.

The MVC measurement begins with two seconds of preparation time in relaxed state before the first contraction. The duration of the rising edge of the trapezoidal feedback is one second. The plateau is three seconds long and the falling edge, similarly to the rising edge, is one second long. The subject has twenty seconds to relax before the next round.

When measuring the MVC's, the subject was asked to perform the eight numbered motions listed in Table 4 to their maximum force level. The motions were performed in the order that the table presents. During the twenty seconds of relaxation, the next motion to be performed was read aloud to the subject.

Figure 24 shows the raw 8 channel data from all the setups on one subject. Visual examination of the graphs reveals that there is a noticeable difference between the motions, but also that each motion measured with different setup is relatively similar. The data also suggests that finger abduction and wrist supination are probably the most difficult to differentiate between in the gesture recognition experiment.

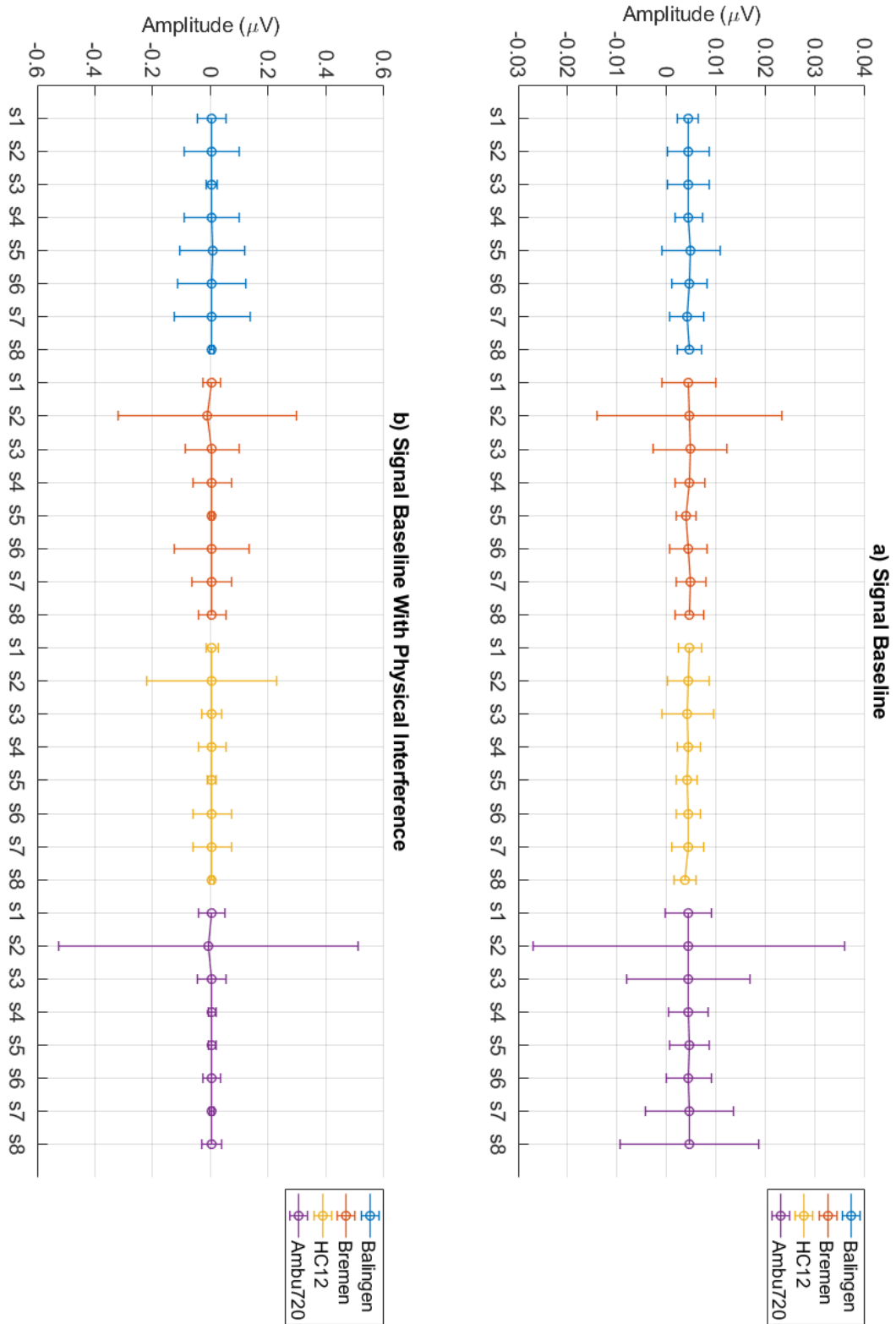


Figure 23: The signal average and standard deviation (error bars) when subject's arm is relaxed. In panel b the subject's forearm was also tapped around the electrodes during the measurement.

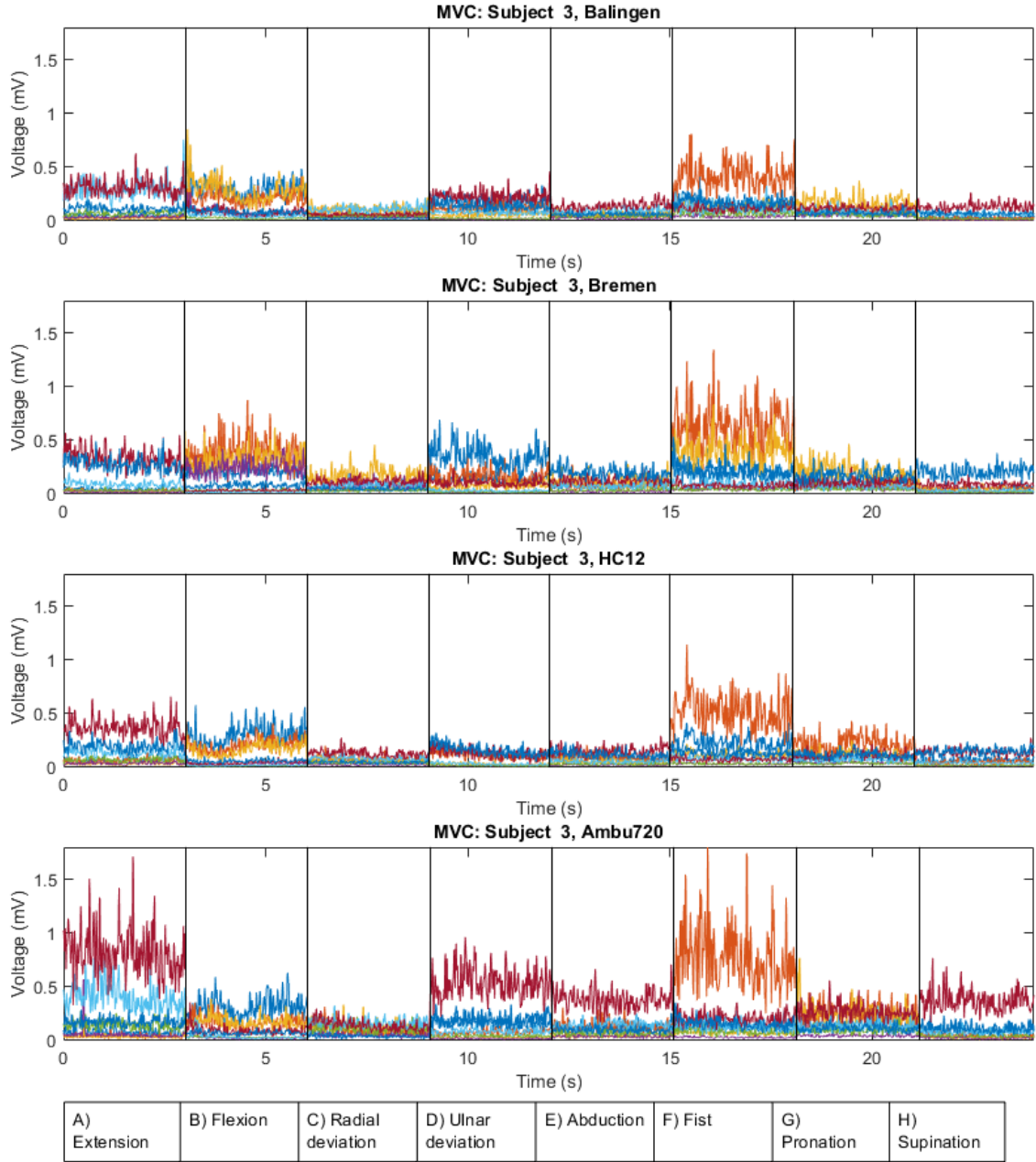


Figure 24: Data from the MVC measurements on one subject, each color representing one channel. The figure only presents the data during the three second plateaus of the trapezoidal feedback of each motion and the data between has been cut out. Root-mean-square (RMS) has been applied to the data with 50 samples window and 25 samples overlapping.

#### 4.3.3 Functional Gesture Recognition Test

In the functionality test, eight subjects were asked to perform five repetitions of the nine motions listed in Table 4 to a comfortable force level, accumulating to 45 motions in total. To compensate for the physical parameters such as the electrode

impedance and the muscle fatigue, the order of the motions was randomized. The motion instructions were given with an animation made with Processing (Processing Foundation, USA). It is a sketchbook software and a programming language that can be used to create visual arts such as digital pictures, animations and games [37]. The program first generates a list that contains five instances of each of the nine predetermined motions and shuffles the order to provide a new sequence every time the code is run. The list is saved to a file so that the motions can be identified and labeled after the recording session. The program then displays one item of the list at a time in parallel with the trapezoidal feedback cue.

Table 4: List of the performed motions when measuring the MVC’s and the functionality. The MVC’s were performed in this order, while the motions were randomized during the functionality test. No movement requires no contraction, so it was not included in MVC measurements.

Label	Motion
1	Wrist extension
2	Wrist flexion
3	Wrist radial deviation
4	Wrist ulnar deviation
5	Finger abduction
6	Hand close
7	Wrist pronation
8	Wrist supination
9	No movement

A machine learning MATLAB script developed by the department of Bionic and Rehabilitation Engineering in Aalto University based on [38] was trained and tested with the data gathered from the gesture recognition experiment. The sections of the data when the trapezoidal feedback is nonzero were isolated and labeled. One data set consists of an eight-channel measurement of one electrode setup on one subject. Each data set was divided into a training and a testing portion. Out of five repetitions for each motion, one was assigned to the testing portion and the remaining four to the training portion. The machine learning algorithm was run five times for each data set, changing which instance of repetition was assigned to the test portion.

Figure 26 presents the results as confusion matrices for each electrode setup. A confusion matrix represents the results of a data classification experiment. Every row includes all instances of one motion and adds up to 1, that is 100% of the instances. For example, the first matrix in Figure 26 that represents the results for Balingen electrodes shows that the machine learning algorithm correctly recognised 91% of the cases where the subject performed a wrist extension (predicted motion is 1 and actual motion is 1). However, in 2% of the cases the algorithm incorrectly recognised a wrist extension as a wrist radial deviation (predicted motion is 3 and actual motion



is 1). The average prediction accuracies were Balingen 88.6%, Bremen 87.3%, HC 87.5% and Ambu720 90.9%.

When evaluating data classification performance, two parameters are of interest: the true positive rate (TPR, Equation 2) and the true negative rate (TNR, Equation 3) [39]. The true positive rate answers the question that of all samples that actually are a certain motion, what proportion was predicted correctly. The true negative rate, on the other hand, is the proportion of all the samples that were not a certain motion were correctly predicted not to be that motion.

$$\text{TPR} = \frac{\text{TP}}{\text{TP} + \text{FN}} \quad (2)$$

$$\text{TNR} = \frac{\text{TN}}{\text{TN} + \text{FP}} \quad (3)$$

Figure 27 plots the TPR and TNR values for each electrode setup. The data consists of the TPR and TNR calculated for each motion and the box plot indicates the median, 25th and 75th percentiles, the extreme data points and the outliers. Ambu720 electrodes have the most consistent prediction accuracy. The mean of the true positive rate across all motions was 0.8966 for Balingen, 0.8782 for Bremen, 0.8841 for HC12 and 0.9152 for the Ambu720s. The mean of the true negative rate similarly was 0.9871 for Balingen, 0.9848 for Bremen, 0.9855 for HC12 and 0.9894 for the Ambu720s. These results would suggest that the Ambu720s perform the best, followed by Balingen, HC12 and Bremen electrodes in that order. Still, it can be concluded that the difference is practically negligible.

The functionality experiment was also conducted for a person with limb impairment, which is the target audience for gesture controlled active prostheses. Unfortunately, the forearm stump geometry was not suitable for the prototype sleeves made for this thesis so the measurement was done only with Ambu720s. The prediction accuracy was consistently worse across all the motion classes, totaling in 55.8% average prediction accuracy. Assumingly, the textile electrodes perform slightly worse than Ambu720s as the other experiments have shown.



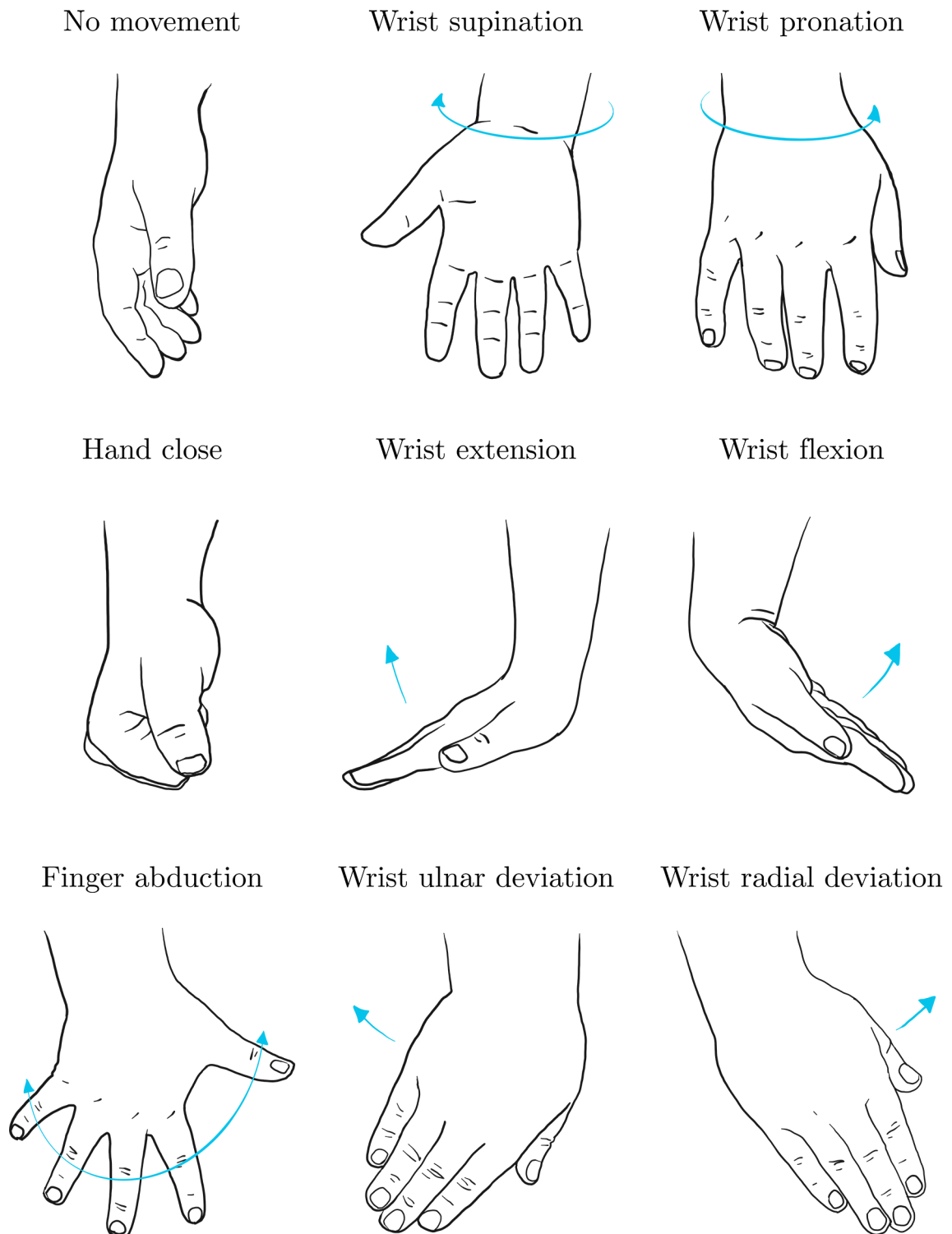


Figure 25: Graphical representations of the motions listed in Table 4. The first two rows of pictures are considered from the frontal plane and the bottom row is showing the sagittal view.

## Action Recognition: Confusion Matrices

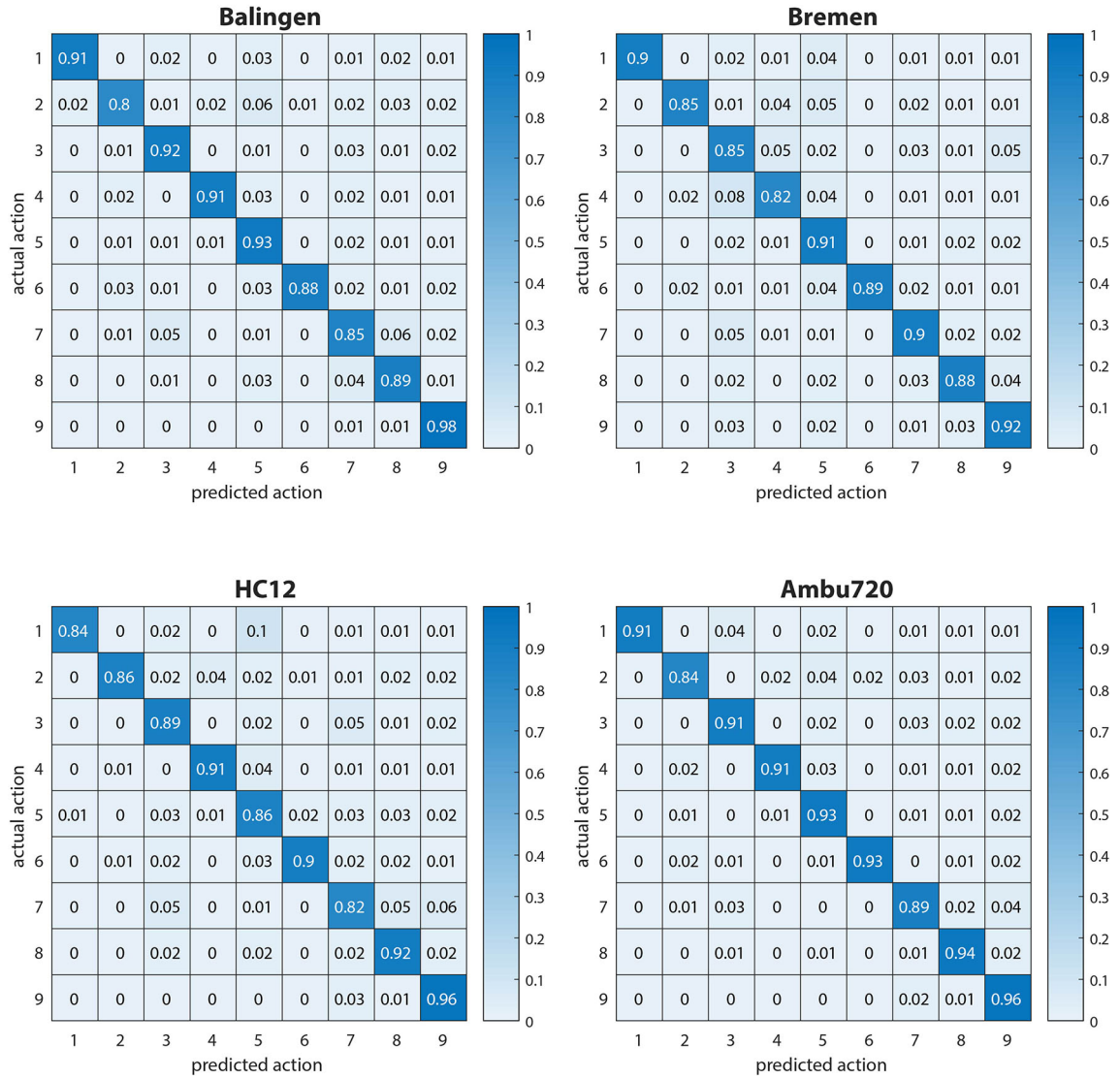


Figure 26: Confusion matrices showing the results of the functionality tests. Each matrix is an average across all subjects measured with one electrode setup. Table 4 lists the motions and their corresponding labels.

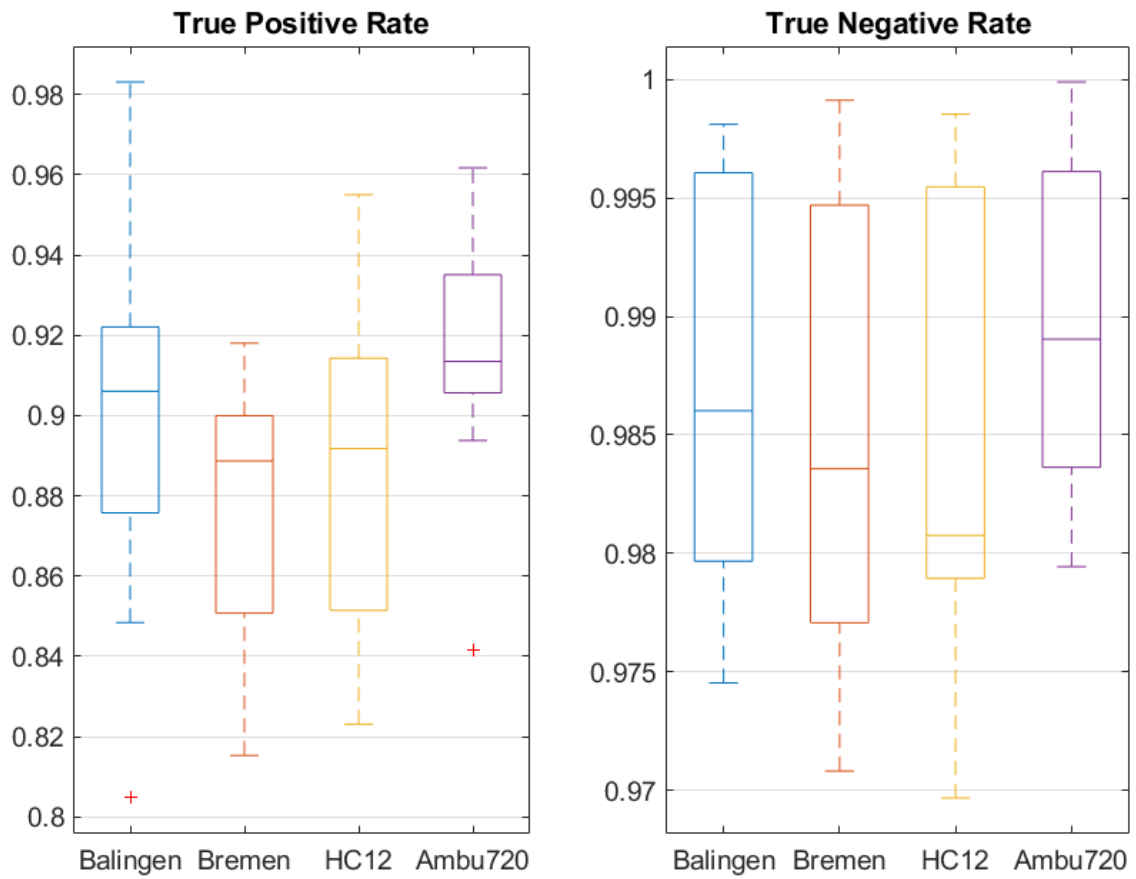


Figure 27: The true positive rate and the true negative rate for each electrode setup across all motions.

## 5 Conclusion

This thesis aimed to evaluate the electric properties of some currently available conductive textile materials. The intention was to investigate their potential to be used as electrodes in the recognition of hand motions from EMG signal for the purpose of establishing intuitive HCI's. The key finding is that the differences between the different conductive materials is marginal and the conventional wet gel electrodes did not perform significantly better in the experiments. Therefore, the best material to be used in making textile integrated surface electrode is the one that is the easiest to work with in the specific application.

Two conductive threads and two conductive fabrics were experimented with to find the optimal electrode design and an efficient and functional work flow while taking into account SENIAM [32] recommendations about electrode size, shape and distance. Two fabrication methods were considered: embroidering the electrodes directly on the base garment with a conductive thread and sewing a piece of conductive fabric onto the base garment.

The embroidering technique proved itself to be very inefficient and the size of the electrodes was the hardest to keep constant. Using the conductive thread as the upper thread and sewing with straight stitch was the only technique that worked for the sports compression sleeve that was used as the base garment. Otherwise the threads broke easily and the sewing machine got jammed. Embroidered electrodes had one clear advantage: there was no issue with the electrode material unraveling, which was a problem especially with Bremen fabric.

The base garment material, unraveling of the electrode fabric and the stitch type used for attaching the electrodes all affected manufacturing the fabric electrodes. An elastic base material posed some challenges with sewing, but not as much as in the case of embroidering with a conductive thread because both upper and bottom thread are non-conductive nylon that is thinner and easier to work with. Unraveling of the fabric made it more difficult keeping the electrodes together in the manufacturing process. The smaller the electrode, the harder it is to work with a fabric that unravels easily. Also, the unraveling tendency might lead to the electrodes breaking faster in the long run.

The electrodes went through three different types of measurements: impedance spectroscopy, frequency response and EMG recording.

Following findings were acquired from impedance spectroscopy. Difference in impedance before and after wetting the electrode is significant. The wet textile electrodes have even lower impedance than the wet gel electrodes, which is desirable but surprising as the wet gel electrodes were assumed to perform better. However, the shapes of the impedance curves suggested that the lower frequencies are more attenuated in wet textile electrodes than dry textile electrodes in relation to higher frequencies, which could change the composition of the EMG signal according to the wetness of the electrodes. Still, the change in the impedance curve shape is small in the frequency range of interest and the amount of overall attenuation when the electrodes dry is likely the main issue. The impedances of the dry textile electrodes were roughly two orders of magnitude larger than the wet gel electrode impedance.

Out of the textile electrodes, Balingen had the lowest impedance when wet, but also the largest impedance when dry. This would suggest the best EMG results when the electrodes remain wet but possibly less consistent results when there are changes in the wetness.

Frequency response measurements revealed that the signal experiences only attenuation from the textile electrodes – no frequency shift or spectral broadening. The results showed no significant difference between the different textiles.

The EMG measurements were performed on eight subjects with an eight channel electrode setup. The measurements consisted of three parts: signal baseline, maximum voluntary contraction (MVC) and functionality. The signal baseline measurements revealed that, aside from subject 2, Ambu720s were the least susceptible to mechanical interference during measurement, but experienced the most noise in calm conditions. Out of the textile electrodes, HC12 experienced the least noise in both cases. The MVC measurement was more of a qualitative check. A visual inspection of the data when performing certain motions gave an inkling of how the signals compare to those measured with Ambu720s. The signals were smaller in amplitude, but similar channels activated in corresponding movements, being promising. The functionality part was the ultimate test. Ambu720s performed the best in the gesture recognition experiment, which was expected. The interesting thing about the results was that the textile electrodes were not far off. The true positive rate of all electrode setups was over 80% and the true negative rate was mostly over 97%. Balingen electrodes performed the best out of the textile electrodes with highest TNR and TPR.

In conclusion, the conductive fabrics available are viable materials for designing EMG electrodes intended for gesture recognition applications. The possibility of using them for more precise biomedical purposes is left for future research to explore. Other future endeavours could include testing the durability and washability of the described garments.

## References

- [1] “What’s the difference between smart and intelligent clothing?” clim8. Accessed on: Mar. 7, 2020. [Online]. Available: <https://www.myclim8.com/2016/12/08/whats-the-difference-between-smart-and-intelligent-clothing/>
- [2] B. Stephenson, “What are smart clothes?” *Lifewire*, Jan. 2020, [Online]. Available: <https://www.lifewire.com/what-are-smart-clothes-4176103>
- [3] R. Hallikainen, “Reiman älyvaatteen lyhyt historia,” *Tekniikka&Talous*, Jan. 2005, [Online]. Available: <https://www.tekniikkatalous.fi/uutiset/reiman-alyvaatteen-lyhyt-historia/4b9a71bb-73eb-3b97-a39a-8f0fde7cec1a>
- [4] ReimaGO. Accessed on: Oct. 6, 2019. [Online]. Available: <https://www.reima.com/fi/reimago/>
- [5] “Occupational health and ergonomics.” Myontec. Accessed on: Oct. 6, 2019. [Online]. Available: [https://www.myontec.com/benefits/occupational\\_health\\_and\\_ergonomics/](https://www.myontec.com/benefits/occupational_health_and_ergonomics/)
- [6] “Suomalaiselle älyvaatteelle uusi urapolku.” VTT. Accessed on: Oct. 6, 2019. [Online]. Available: <https://www.vtt.fi/medialle/uutiset/suomalaiselle-%C3%A4lyvaatteelle-uusi-urapolku>
- [7] S. E. Nishi, R. Basri, and M. K. Alam, “Uses of electromyography in dentistry: An overview with meta-analysis,” *European journal of dentistry*, vol. 10, no. 3, pp. 419–425, 2016. Available: <https://www.ncbi.nlm.nih.gov/pubmed/27403065>
- [8] C. J. D. Luca, “The use of surface electromyography in biomechanics,” *Journal of Applied Biomechanics*, vol. 13, no. 2, pp. 135–163, 1997. Available: <https://journals.humankinetics.com/view/journals/jab/13/2/article-p135.xml>
- [9] W. S. Marras, “Industrial electromyography (emg),” *International Journal of Industrial Ergonomics*, no. 6, pp. 89–93, 1989. Available: [https://spine.osu.edu/files/uploads/Publications/1990/InternationalJournalOfIndustrialErgonomics\\_1990\\_6\\_89-93.pdf](https://spine.osu.edu/files/uploads/Publications/1990/InternationalJournalOfIndustrialErgonomics_1990_6_89-93.pdf)
- [10] R. Ashan, M. I. Ibrahimy, and O. O. Khalifa, “Emg signal classification for human computer interaction: A review,” *European Journal of Scientific Research*, vol. 33, no. 3, pp. 480–501, 2009. Available: <https://pub.uni-bielefeld.de/download/2610087/2645613/jsai-05.pdf>
- [11] T. Batista, L. dos Santos Machado, A. M. G. Valenca, and R. M. de Moraes, “Farmyo: A serious game for hand and wrist rehabilitation using a low-cost electromyography device,” *International Journal of Serious Games*, vol. 6, no. 2, pp. 3–19, Jun. 2019. Available: <http://dx.doi.org/10.17083/ijsg.v6i2.290>
- [12] L. Sherwood, *Human Physiology: From Cells to Systems*, 6th ed. Thomson Brooks/Cole, 2007.

- [13] W. Ganong, *Review of Medical Physiology*, ser. LANGE Basic Science. Mcgraw-hill, 2005. Available: <https://books.google.fi/books?id=OLa8vDBXDD4C>
- [14] R. Merletti and D. Farina, *Surface Electromyography: Physiology, Engineering and Applications*. John Wiley & Sons, Inc., Hoboken, New Jersey, 2016.
- [15] J. Webster, *Medical instrumentation: application and design*, 4th ed. John Wiley & Sons, Inc., Hoboken, New Jersey, 2010.
- [16] R. Seppänen, L. Mannila, M. Kervinen, I. Parkkila, P. Konttinen, L. Karkela, P. Meriläinen, and T. Yli-Kokko, *MAOL-taulukot : matematiikka, fysiikka, kemia*, 6th ed., t. Karinen, Kirsi, Ed. Helsinki: Otava, 2013.
- [17] E. Kappenman and S. Luck, “The effects of electrode impedance on data quality and statistical significance in erp recordings,” *Psychophysiology*, Sep. 2010. Available: <http://dx.doi.org/10.1111/j.1469-8986.2010.01009.x>
- [18] L. M. Castano and A. B. Flatau, “Smart fabric sensors and e-textile technologies: a review,” *Smart Materials and Structures*, vol. 23, no. 5, p. 053001, apr 2014. Available: <https://doi.org/10.1088%2F0964-1726%2F23%2F5%2F053001>
- [19] H. Kuhn, W. Kimbrell, J. Fowler, and C. Barry, “Properties and applications of conductive textiles,” *Synthetic Metals*, vol. 57, no. 1, pp. 3707 – 3712, 1993, proceedings of the International Conference on Science and Technology of Synthetic Metals. Available: <http://www.sciencedirect.com/science/article/pii/S037967799390501M>
- [20] D. Knittel and E. Schollmeyer, “Electrically high-conductive textiles,” *Synthetic Metals*, vol. 159, no. 14, pp. 1433 – 1437, 2009. Available: <http://www.sciencedirect.com/science/article/pii/S0379677909001659>
- [21] A. Lansdown, “Silver in health care: Antimicrobial effects and safety in use,” *Biofunctional Textiles and the Skin. Curr Probl Dermatol.*, vol. 33, pp. 17–34, jun 2006.
- [22] S. Yang, P. Premaratne, and P. Vial, “Hand gesture recognition: An overview,” in *2013 5th IEEE International Conference on Broadband Network Multimedia Technology*, Nov 2013, pp. 63–69.
- [23] C. Amma, T. Krings, J. Böer, and T. Schultz, “Advancing muscle-computer interfaces with high-density electromyography,” in *Proceedings of the 33rd Annual ACM Conference on Human Factors in Computing Systems*, ser. CHI '15. New York, NY, USA: ACM, 2015, pp. 929–938. Available: <http://doi.acm.org/10.1145/2702123.2702501>
- [24] S. S. Rautaray and A. Agrawal, “Interaction with virtual game through hand gesture recognition,” in *2011 International Conference on Multimedia, Signal Processing and Communication Technologies*, Dec 2011, pp. 244–247.

- [25] G. Murthy and R. Jadon, “A review of vision based hand gesture recognition,” *International Journal of Information Technology and Knowledge Management*, vol. 2, pp. 405–410, 08 2009.
- [26] S. Benatti, B. Milosevic, F. Casamassima, P. Schönle, P. Bunjaku, S. Fateh, Q. Huang, and L. Benini, “Emg-based hand gesture recognition with flexible analog front end,” in *2014 IEEE Biomedical Circuits and Systems Conference (BioCAS) Proceedings*, Oct 2014, pp. 57–60.
- [27] D. Farina, T. Lorrain, F. Negro, and N. Jiang, “High-density emg e-textile systems for the control of active prostheses,” in *2010 Annual International Conference of the IEEE Engineering in Medicine and Biology*, Aug 2010, pp. 3591–3593.
- [28] G. R. Naik, D. K. Kumar, and Jayadeva, “Twin svm for gesture classification using the surface electromyogram,” *IEEE Transactions on Information Technology in Biomedicine*, vol. 14, no. 2, pp. 301–308, March 2010.
- [29] S. Amsüss, L. P. Paredes, N. Rudigkeit, B. Graimann, M. J. Herrmann, and D. Farina, “Long term stability of surface emg pattern classification for prosthetic control,” in *2013 35th Annual International Conference of the IEEE Engineering in Medicine and Biology Society (EMBC)*, July 2013.
- [30] Statex. Accessed on: Mar. 29, 2020. [Online]. Available: <https://statex.de/en/>
- [31] *Instruction Manual OEKAKI 50 Oekaki Series*.
- [32] The SENIAM project. Accessed on: Sep. 16, 2019. [Online]. Available: <http://www.seniam.org/>
- [33] A. Gruetzmann, “Novel dry electrodes for ecg monitoring,” *Physiol. Meas.* 28, pp. 1375–1390, Mar 2007. Available: <http://doi.org/10.1088/0967-3334/28/11/005>
- [34] Ambu, “Ambu neuroline 720 datasheet,” [https://www.ambu.com/Admin/Public/DWSDownload.aspx?File=%2fFiles%2fFiles%2fDownloads%2fAmbu+com%2fNeurology%2fEMG\\_electrodes%2fNeuroline+720%2fDatasheets%2fIE\\_Neuroline\\_720\\_Datasheet\\_v04\\_493772001.pdf](https://www.ambu.com/Admin/Public/DWSDownload.aspx?File=%2fFiles%2fFiles%2fDownloads%2fAmbu+com%2fNeurology%2fEMG_electrodes%2fNeuroline+720%2fDatasheets%2fIE_Neuroline_720_Datasheet_v04_493772001.pdf), 2019.
- [35] Audacity. Accessed on: Jun. 29, 2019. [Online]. Available: <https://www.audacityteam.org/>
- [36] B. Peacock, T. Westers, S. Walsh, and K. Nicholson, “Feedback and maximum voluntary contraction,” *Ergonomics*, vol. 24, no. 3, pp. 223–228, 1981. Available: <https://doi.org/10.1080/00140138108559236>
- [37] Processing. Accessed on: Dec. 16, 2019. [Online]. Available: <http://processing.org>



- [38] K. Englehart and B. Hudgins, “A robust, real-time control scheme for multi-function myoelectric control,” *IEEE Transactions on Biomedical Engineering*, vol. 50, no. 7, pp. 848–854, 2003.
- [39] H.-m. Shim, H. An, S. Lee, E. H. Lee, H.-k. Min, and S. Lee, “Emg pattern classification by split and merge deep belief network,” *Symmetry*, vol. 8, no. 12, 2016. Available: <https://www.mdpi.com/2073-8994/8/12/148>